LAWRENCE
LIVERMORE
NATIONAL
LABORATORY

UCRL-JRNL-232824

Properites of ultrathin films appropriate for optics capping layers in extreme ultraviolet lithography (EUVL)

S. Bajt, N. V. Edwards, T. E. Madey

July 18, 2007

Surface Science Review

Properties of ultrathin films appropriate for optics capping layers in extreme ultraviolet lithography (EUVL)

S. Bajt[a], N. V. Edwards[b] and T. E. Madey[c]

[a] Physics and Advanced Technologies, Lawrence Livermore National Laboratory, Livermore, CA, USA

[b] Freescale/SEMATECH, Austin, TX, USA

[c] Department of Physics and Astronomy, Rutgers University, Piscataway, NJ 08854, USA

Abstract

The contamination of optical surfaces by irradiation shortens optics lifetime and is one of the main concerns for optics used in conjunction with intense light sources, such as high power lasers, 3rd and 4th generation synchrotron sources or plasma sources used in extreme ultraviolet lithography (EUVL) tools. This paper focuses on properties and surface chemistry of different materials, which as thin layers, could be used as capping layers to protect and extend EUVL optics lifetime. The most promising candidates include single element materials such as ruthenium and rhodium, and oxides such as TiO_2 and ZrO_2.

Keywords: Optics contamination, protective film, capping layer, multilayer, extreme ultraviolet, extreme ultraviolet lithography, oxidation, carbonization, ruthenium, rhodium, TiO_2, ZrO_2

1. Introduction

1.1 Background

The semiconductor industry is driven by Moore's law[1], which predicts that the number of transistors on a microprocessor doubles every 18 months. The smallest feature size currently (2007) produced in volume fabrication is 65 nm obtained with 193 nm and 248 nm wavelength of light. Although fabrication of sub-wavelength features is possible utilizing various effects such as immersion techniques and phase-shifting masks, additional minimizing requires a shift to even shorter wavelengths. Extreme ultraviolet lithography (EUVL), using 13.5 nm wavelength, has emerged as one of the most promising next generation lithographic techniques. Radiation at these short wavelengths is strongly absorbed by any matter and therefore the EUVL tools need to operate in vacuum. Also, lenses used in traditional optical lithography have to be replaced with multilayer-coated[2] reflective optics with high EUV reflectivity and wavelength selectivity.

The basic principle behind the multilayer mirror is simple. A multilayer is an artificial structure with a large number of interfaces (Figure 1). A single interface reflects a small fraction of an incident beam. However, the reflectivity increases dramatically if the reflected beams from all the interfaces in the multilayer add in phase. Multilayers obey Bragg's law which means that constructive interference occurs for a given wavelength and angle of incidence if the layer thicknesses are properly chosen. The highest reflectance is usually achieved by choosing materials with the largest difference in their refractive indices and extinction coefficients. This means that one material is more

absorbing (absorber) while the other material is more transparent (spacer). For the EUV range the best material pair seems to be Mo and Si.

EUV reflective optics consist of precisely figured substrates coated with alternating layers of Mo and Si. A multilayer pair or unit consists of one Mo and one Si layer and is only about 7 nm thick. A typical multilayer consists of 40-60 repeats of this unit and usually ends with a Si layer, which partially oxidizes when exposed to the air. Individual layer thicknesses in the EUV multilayer are about 2.8 nm for Mo and 4.2 nm for Si, respectively.

In the EUVL tools, with a vacuum of about 10^{-5} Pa, the surfaces of such multilayer-coated mirrors are exposed to EUV radiation in the presence of residual contaminants (primarily water vapor and hydrocarbons), which leads to optics contamination (oxidation and carbon deposition). At EUV wavelengths even a small increase in oxide or carbon layer of only few nm causes a measurable reflectivity decrease. Yet, reflectivity has to be stable within 1% in high volume manufacturing (HVM) lithography because the optical throughput is proportional to:

$$\int \prod_{i}^{n=1} R^{i}(\lambda) d\lambda \quad (1)$$

where R is the reflectance of the i^{th} multilayer mirror and n is the number of reflective mirrors in the EUVL tool (Figure 2). These HVM tools might contain 9 or more reflective mirrors and any small change in reflectivity will lead to a noticeable change in their throughput. Hence, optics lifetime is one of the critical issues for the success of this

technology and different strategies to impede oxidation and contamination[3,4,5,6,7,8] have been studied. One way to extend the lifetimes of the projection optics is by coating the multilayers with thin (~ 2 nm) capping layer[9,10,11,12,13,14,15] films (Figure 1) that reduce the build-up of contamination. In this paper we evaluate most of the solid phase elements in the periodic table and their material combinations as possible capping layer candidates for EUVL applications.

In addition to the aforementioned application in the semiconductor industry[16,17,18,19] these high-reflectivity multilayer mirrors enabled a new class of telescopes for solar physics and astronomical research[20,21,22,23], are being used as diagnostic elements in laser science and research,[24] as focusing Kirkpatrick-Baez[25] mirrors, and zone plates in soft x-ray microscopes[26,27,28,29,30] and as hard x-ray microscopes at synchrotron facilities.[31,32] Recently, multilayers also enabled breakthrough experiments in free electron laser (FEL) applications.[33,34,35,36,37]

1.2 Motivation and Objectives

The HVM tools for EUVL require optics with 30,000 light-on hours of lifetime. This represents 10 years of continuous use.[38] Other examples, where Mo/Si multilayers operate in a similar wavelength region and require long optics lifetimes, are mirrors on the Extreme-Ultraviolet Imaging Telescope (EIT)[39] on SOHO that is being used for imaging solar corona[20] and mirrors on the Transition Region and Coronal Explorer (TRACE)[22], whose primary mission is to study magnetic fields and the associated plasma

structures on the Sun. Both SOHO's EIT and TRACE instruments are still working after 11 and 8 years in space, respectively. However, the space optics operates in somewhat different environment than the optics for EUVL applications. The main concern for space optics is their stability at slightly elevated temperature[40] and the effect of O atom bombardment, a likely environment for optics used in satellite instruments in lower Earth orbit. Since the temperature in EUVL exposure tools needs to be extremely stable the thermal effects on projection optics coatings should be negligible. Carbon contamination on mirror surfaces irradiated with short wavelength radiation is also a well known problem in the synchrotron and laser communities.[41] Different carbon cleaning procedures, on- and off-line, have been successfully implemented without noticeable loss in mirror reflectivity.[42,43,44,45,46]

The EUVL exposure tools with high power ionizing photon sources operate in ~10^{-5} Pa vacuum. The traditional strategies for obtaining and maintaining ultra-high vacuum cannot be used in these tools so the residual water and other contaminants in the presence of EUV photons oxidize and degrade the optics surface. Both oxidation and carbon deposition on the optical surfaces reduce the reflectivity of the optics and can introduce wavefront aberrations. The overall effect is not only the reduction in the throughput of the exposure tool but also a reduction in printing uniform features[47]. Despite recent progress obtained by the combination of oxidation-resistant capping layers and *in situ* cleaning strategies that attempt to leverage chamber gas-surface interactions to impede oxidation and contamination[48,49,50,51,52,53], optics lifetimes still fall short of specifications for high volume manufacturing by nearly two orders of magnitude. Hence, the short EUV

(13.5 nm) wavelength creates a range of technological challenges not present in the traditional lithographies. The EUV optics researchers, confronted with the failure of phenomenological approaches to extend optics lifetime, are now finding themselves occupied with fundamental surface science[54,55] to understand the range of gas/surface interactions possible for projection optics rather than with the development of detailed manufacturing specifications or lifetime test protocols, as originally expected. To develop a commercially viable EUVL exposure tool, workers must create a stable process window for *in situ* optics cleaning that strikes the appropriate balance between carbon deposition and oxidation by finding the "right" combination of protective capping layer and projection optics chamber background gases. In an ideal world, a judiciously chosen material would allow EUV lithographers to altogether avoid one or the other destructive processes. A neat and tidy solution of this kind has not yet materialized; this means that it is necessary to undertake a survey of broad range of existing materials and to subject them to optics performance criteria. These have evolved over the past several years while attempting to understand the degradation of and to elucidate the structure-function relationship for EUV optics capping layers.

The paper follows our thought process. We first introduce the design criteria of the ideal capping layer candidates where both optical and structural (surface) properties are equally important. Then we simulate the optical performance for all solid phase elements and material combinations for which we have available optical constants. The simulations assume these candidates being deposited on the top of the multilayer stack with ideal properties (full coverage, no roughness, no interdiffusion, etc.). Only the candidates that

satisfy the gating/evaluation criteria (adding the capping layer causes < 1% reflectivity drop for pure elements and <2% reflectivity drop for compounds) are evaluated further for their surface chemistry performance. In particular we consider their chemical stability and various aspects of their surface reactivity including radiation damage and thermal stability. The environmental health and safety concern are briefly discussed in a separate section. Once the best materials are selected based on these gating criteria we discuss how to actually make them. Possible ways are described in sections on thin film fabrication and vacancy management. We conclude with a summary of our findings and proposed solutions.

2. Design Criteria

2.1 Optical Properties

Recent research concerning degradation mechanisms of EUV optics[12,54] has refined the concept of what comprises a successful protective capping layer. To a large extent the design criteria have evolved with the state of knowledge concerning capping layer surface chemistry and nanostructure. Certain requirements are largely self-evident especially those that pertain to optical performance and specifications for producing smooth, continuous films.

First, a suitable protective capping layer for EUV optics must have optical properties such that the reflectivity (at λ = 13.5 nm) of the entire multilayer interference coating, capping layer included, does not drop below a level that would render it unsuitable for

lithographic purposes. In theory this would seem to enable many of a number of material designs but in practice researchers are severely inhibited by the requirement that the film in question must also be made continuous and smooth (~0.2 nm high spatial frequency roughness) over only several nanometers of thickness, in order that the EUV reflectivity of the film stack is preserved. Indeed, in this work, it is apparent that only two nanometers—in a few cases, three—of capping layer material can be tolerated. If this were not sufficiently challenging, this capping layer must also be deposited at low growth temperatures (<200° C) to avoid intermixing with the underlying multilayer mirror stack.

2.2 Structural (Surface) Properties

The optical design criteria do not include the nanoscale capping layer properties and complex surface chemistry that must be coordinated in order to prevent degradation of the layers. Until relatively recently, it was not clear that reactivity with respect to C and O was the crucial gating criterion. Ideally, the surface of the material should be engineered such that C and O atoms are induced to recombine on optics surfaces to form CO or CO_2, which could then be desorbed thermally or by electron- or photon-stimulated desorption processes associated with the incident EUV flux. Or, these mechanisms could be exploited in a hydrocarbon-rich environment by introducing water vapor or other oxidizing gases in appropriate amounts to minimize carbon deposition. In practice, how to do this for a given material and microstructure is not clear. Candidate capping layers must be coordinated with background chamber gases to strike the appropriate balance between carbon and oxide deposition, while also being designed to be sufficiently dense

to prevent the uptake of oxygen or other contaminant molecules. If the capping layer is polycrystalline, this layer of nanometer-scale thickness should have a grain structure/crystallographic texture that curtails the diffusion of oxygen through the layer. If amorphous—indeed, regardless of the structure—these capping layers must also be free of defects (such as mobile vacancies or dislocations) that would allow for oxygen diffusion through the layer. Films must be chemically inert with respect to the stack materials underneath, they must be thermally stable, and they also must generate minimal stresses in the film stack during deposition.[9,10,11] Finally, EUV optics capping layers must not be prohibitive in terms of cost or require violations of common environmental, health and safety regulations during their manufacture and use.

3. Gating/Evaluation

In this evaluation, the goal is to take a fresh look at the periodic table and evaluate the solid phase elements first, followed by other material combinations, according to the design criteria described previously. However, by doing so it is not meant to imply that there has not been previous materials research concerning multilayer and capping layer development (acknowledging that much of the knowledge about materials that has been marshaled to solve the capping layer problem was originally obtained in the context of multilayer development). For a history of such activities at Lawrence Livermore National Laboratory (LLNL), in the context of EUVLLC[56] and LITH160 SEMATECH funding, see Appendix A. Given that the majority of early ground breaking work in this area was done by LLNL, this history should provide the reader with a good picture of relevant

milestones. For both seminal and recent developments from other researchers the following references are useful.[57,58,59,60,61,62,63,64,65,66,67,68,69]

3.1 Optical Performance

In theory, it should be simple to evaluate the EUV optical properties of materials to determine their suitability as capping layers but in practice, this exercise is not trivial. To evaluate the impact of a thin candidate capping layer on a Mo/Si multilayer mirror EUV reflectivity optical constants of materials under evaluation are required. Unless already available this involves the fabrication of a specialized set of samples, which by itself can require significant materials development. Without direct evidence that a new material has the necessary EUV optical properties to merit consideration as a capping layer, there is often little motivation to invest in expensive development activities to produce the samples for optical constant determination.

Indeed, there is a lack of reliable optical constants in the EUV region and the most commonly used optical constants are derived from calculated atomic scattering factors.[70] There are large discrepancies among data reported by different researchers on the same material because of a number of difficulties inherent to the EUV range. Strong absorption, especially above the absorption edges prevents reliable transmission measurements unless very thin unsupported films can be fabricated and a radiation source with high photon flux and spectral purity is available. Most of the experimental data collected in the past suffer from errors or uncertainties due to poor sample preparation such as contamination, surface roughness and poor source quality. To experimentally

determine optical constants one needs to fabricate a specialized set of samples and to have access to a radiation source with high photon flux and spectral purity, such as a synchrotron source.

The most frequently used methods to determine optical constants are transmission, interferometry, reflectance, ellipsometry and angle-dependent electron yield. Angle-dependent reflectance measurements have the advantage that both the real and imaginary parts (δ and β) can be deduced experimentally, and the measurements can be performed on bulk samples without the need to fabricate free-standing thin films.[71] However, this method has also possible pitfalls, which include its sensitivity to surface roughness, sample quality and contamination. Ellipsometric measurements in the EUV spectral range also suffer from the lack of suitable polarizer materials, as MgF_2, the common polarizer choice for VUV instruments, absorbs above ~9.5 eV; the gold prism polarizers typically used for measurements above 9.5 eV have serious non-idealities that compromise data quality.[72] The other commonly used method to obtain optical constants is to deduce the absorption coefficient from both transmission measurements and theoretical calculations.[73,74,75] The real part of *n* is then calculated through Kramers-Kronig relations. Transmission measurements require thin, self-supporting films, which are difficult to fabricate and are sensitive to contamination. Film thickness is a necessary and important input parameter.

If optical constants are obtained of *in-situ* deposited films then it is possible to avoid contamination due to air exposure. In practice, very few materials have been analyzed

this way.[76] More often, the optical constants are derived from transmission and reflectance measurements of films exposed to air. To minimize contamination, films can be protected with less reactive material, such as carbon. Or they can be sandwiched between two carbon layers in the case of free-standing films for transmission measurements. Sandwiched films are also more robust and easier to handle. Another method is to sputter material directly on thin Si_3N_4 membrane[74,75] and measure transmission through both the material and the membrane. If the optical constants are derived from transmission measurements a set of at least three different thickness films is required although more data points are desirable. At each energy, the absorption coefficient, μ, is inferred from the slope of the transmission versus material thickness curve (on a logarithmic scale).[77,78]

When designing optical constant experiments it is important to choose material thicknesses such that films remain transparent for energies of interest and that the transmission vs. material thickness results in clearly separated curves. In the EUV region this requires films with thicknesses between 15 and 200 nm. When extracting optical constants from these measurements it is important to understand the effects of sandwich layers or support membranes (which will cause alterations in the measurements) and to properly account for them. Parameters such as membrane and sandwich thickness and density need to be known. It is also important that the materials are chemically homogenous and uniform in thickness. For novel compounds, to fabricate such films can require a full materials development effort.

To determine the suitability of candidate materials in this study, we first extracted information on densities (ρ), delta (δ), beta (β) and attenuation lengths at 13.50 nm (91.84 eV) for pure elements (Z = 1- 92) and for compound materials (for which optical constants exist) from the CXRO[79] web page. Using CXRO densities we then calculated the reflectivity (see Appendix B) of a 50 bilayer Mo/Si multilayer with a period thickness of 6.91 nm (Si layer thickness = 4.146 nm and Mo layer thickness = 2.764 nm). The calculation assumed a perfect multilayer structure (no roughness, interdiffusion or surface oxide), and it was performed for normal incidence angle (0 degree) in a vacuum ambient and assuming that the substrate was a Si wafer with 0.1 nm surface roughness. The calculation was carried out for the wavelengths between 13.0 and 14.0 nm with 0.01 nm step size assuming unpolarized incident light and perfect instrumental resolution.

Since it is not always obvious which element or compound should be used as a spacer and which as an absorber layer we calculated two cases: in the first the capping layer material under consideration was placed on top of a terminating Si layer; in this case, the first layer of the multilayer was Mo. In the second case, the capping layer was placed on the top of the final Mo layer. Here the multilayer began with a Si layer. However in both cases the calculation assumed a multilayer stack with 50 bilayers. To demonstrate the large sensitivity of the total stack reflectivity to terminating layer thickness, we calculated reflectivity for three different capping layer thicknesses: 2 nm, 3 nm and 4 nm, respectively. Since the maximum reflectivity peak did not always coincide with 13.50 nm wavelength due to different optical constants of the capping layers we decided to report three numbers: reflectivity at 13.50 nm, the peak wavelength (in nm) and the maximum

peak reflectivity at peak wavelength. The maximum peak reflectivity and the 13.5 nm reflectivity are typically off by only ± 0.1 nm and very rarely the difference in reflectivity exceeds 1%, which is much less than uncertainties in the optical constant values. It is straightforward to design a multilayer where the maximum peak reflectivity and the reflectivity at 13.50 nm coincide by adjusting the capping layer thickness. To be considered as a viable capping layer, elemental materials were allowed to cause a drop in reflectivity for the entire film stack of ~1 % or less and ~2% or less was allowed for compounds. The different criteria for elements vs. compounds was used because of the relatively larger uncertainties in the calculated (vs. experimentally determined) optical constants for compounds.[80]

Reflectivity calculation results for non-gaseous elemental and compound materials that meet these criteria are summarized in Tables 1 and 2, respectively. Negative values for $\Delta R = R(Si) - R(max)$ are observed for some materials and indicate that the addition of a capping layer of that thickness results in a slight increase in reflectivity. Complete results of the reflectivity calculations for all of the materials under consideration are given in the Appendix C (Tables C1, C2, C3 and C4: Table C1 features results for elemental materials deposited on a terminating layer of Mo; Table C2, results for elemental materials deposited on a terminating layer of Si; Table C3, results for compound materials on Mo, and Table C4, results for compound materials on Si. Note that the list of compounds available at the CXRO website is by no means exhaustive. In fact, calculated optical constants are only available for a relatively small subset of compound materials, as opposed to the relatively comprehensive compilation of information for elements in

Henke, et al.[81] Accordingly, we decided that if a class of materials appeared promising from a surface chemistry perspective, that it would be evaluated as candidates from the point of view of the other gating criteria even if optical performance were unknown. Of course, if the material appears promising in all other aspects it is recommended to fabricate films to measure its optical constants experimentally and determine whether the material is indeed worth a full capping layer development effort.

3.2 Surface Chemistry Considerations in Choice of Capping Layer

3.2.1 Background

Based on the optical constant data presented in Tables 1 and 2 and discussed in the previous section, we can identify potential candidate materials for capping layers. In the following discussion we separate these materials into (a) elements, (b) binary compounds (mostly oxides and carbides) and (c) ternary compounds and beyond. We focus on the chemical stability of such materials as thin films, and consider various aspects of the surface reactivity.

First, we consider the stability of the films when exposed to atmospheric air. The films will be deposited in vacuum, but at some point they will invariably be exposed to air with some moisture content. Many materials with favorable optical properties fail this first screening, due to rapid oxidation, hydroxide or carbonate formation which can compromise the film's optical, physical and chemical integrity (e.g, alkali and alkaline earth metals). Even films that are not completely oxidized will have surface layers

affected by air exposure. Film microstructure (amorphous, polycrystalline, etc.) will affect reactivity.

Second, we need to consider the films' reactivity during prolonged exposure to background vacuum gases (mainly H_2, H_2O, CO, CO_2, hydrocarbons). Important processes include deposition of carbon, reactions that accelerate growth of oxides, carbides, and oxycarbides, etc.

Third, the effects of EUV radiation-induced processes are important. Different physics is involved in different processes (indirect and direct excitations). The radiation-induced dissociation of adsorbed background gases and the reactivity of atomic and radical fragments are affected most strongly by indirect processes, i.e., low-energy secondary electrons released from the substrate during irradiation by EUV photons. Cross sections (dissociation probabilities) for molecular dissociation are very high for low energy electrons (< 10 eV). In contrast, direct processes involving photoexcitation of substrate core[82] electronic levels by EUV photons are well known to cause photon-stimulated desorption (PSD) of O from oxides, which can affect the stoichiometry, lifetime and surface chemistry of such materials.

Fourth, aspects of mitigation should be considered: e.g., how might one inhibit the growth of oxides, carbides, etc. by adjusting gas mixtures during exposure to EUV radiation? A related topic concerns possible removal of built-up carbon layers, or

reduction of oxides. Atomic hydrogen has been shown to be effective for cleaning both C and O from certain surfaces.

Finally, we note that most of the surface science literature concerning elements and compounds focuses on well-characterized single-crystal sample surfaces. In the present paper, we must extrapolate from the ideal properties of monocrystalline surfaces to the behavior of thin films that can be amorphous or polycrystalline, with potentially high concentrations of defects and vacancies. Much of this is unknown territory, especially for compounds. This is a daunting task!

3.2.2 Elemental Materials with [R (Si) - Rmax] < ~1. 0

The following non-gaseous elements are considered; they are identified by their row of the periodic table. All of these have favorable optical properties as capping layers (2 nm) when covering Si as the top layer (Figure 3).

2^{nd} row: Li, Be, B, C

3^{rd} row: Si, P, S

4^{th} row: K, Ca, Sc, Ti, V

5^{th} row: Rb, Sr, Y, Zr, Nb, Ru, Rh, Pd

6^{th} row and Rare Earths: Ba, La, Ce, Pr, Nd, Pm, Sm, Eu

Actinides: U

Certain materials are clearly *inappropriate* when deposited as elemental films. Alkalis and alkaline earths (Li, Be, K, Ca, Rb, Sr, Ba) react aggressively with oxygen in the air.

All of these metals, and their oxides, are also reactive with water vapor and CO_2, and can form hydroxides and carbonates. When metals films react to form oxides and hydroxides, flaking and scaling of films can occur. In addition, Be vapor and dust are poisonous.

C films are poor choices - C can react with atomic O and H in EUV exposure tools and be removed from the surface. P and S are very reactive and inappropriate.

It is generally accepted in the EUV community that Si or Mo are too reactive in water vapor + EUV to be useful as capping layers. Note that atomically clean Si, upon exposure to air, forms a "native oxide" layer about 1 nm thick. Further growth of oxide (or carbide) can take place under EUV exposure tool conditions, and its rate is affected by film microstructure.

The rare earths (La, Ce, Pr, Nd, Pm, Sm, Eu) are also very reactive in air, and with O-containing vacuum gases (H_2O, CO). Rare-earth metals are known to quickly tarnish in air, and can form an oxide that spalls off and exposes the metal to further oxidation. Uranium is an interesting possibility, but handling large amounts of radioactive material (even depleted U) is not practical, and may not be legal.

Whereas many elemental films appear to be undesirable, some of the above elements are less reactive in various compounds (e.g, perovskite materials $BaTiO_3$, $SrTiO_3$, $ScDyO_3$), and are considered below. Further information concerning the reactivity of relevant elements with oxygen is presented in Appendix D.

Elements that should be considered further are:

4^{th} row: Sc, Ti, V,

5^{th} row: Y, Zr, Nb, Ru, Rh, Pd

Sc, Ti, V: Metal films of all three react with air and water vapor to form films of oxides and/or hydroxides. As in the case of Si or Al,[1 - Footnote] it is likely that a limiting thickness ~ 1nm is formed at 300K, with further growth under EUV conditions. The net increase in film thickness as reactive layers are formed will have an influence on the resultant reflectivity. TiO_2 is already undergoing extensive testing and shows some promise. A question concerns O diffusion through the metals and oxides, and the role of grain boundaries. Oxides of V are good CO oxidation catalysts even at 300K in a radiation environment; the mechanism involves reaction of CO with lattice O to form a vacancy. Oxides of all three will experience radiation damage - see below. All three form stable carbides.[83]

Y, Zr, Nb: These elements are very reactive and form oxides that are good ionic conductors under certain conditions (O-diffusion at elevated T), and can be O storage materials. The oxides are not readily reducible by H or H_2. Nb also forms an oxide more readily than Ru, Rh, and Ir. All three (Y, Zr, Nb) form stable carbides.[83]

[1] The optical performance of Al in the calculations of Section 4.1 eliminated it as a serious contender for a capping layer. A two nanometer film of Al on a Si-terminated Mo/Si multilayer (50 bilayers) resulted in a 3.12% drop in reflectivity. The performance of Ir in this regard was substandard as well, with a drop in R of 1.74% for the same conditions.

The three metals Ru, Rh, Ir[2 - Footnote] are attractive insofar as thin films deposited in vacuum can undergo air exposure and remain metallic. In addition, they do not react significantly with H_2O vapor. Ru forms ultrathin oxide films with (relatively) low heats of formation per O atom. Bulk oxidation of Ru does not occur spontaneously upon exposure to O-containing gases at 300K, and the oxygen-covered surface can be reduced by H-atoms. Many aspects of the surface chemistry of Ru in EUV applications have been discussed by previous workers.[54] Rh and Pd have many of the virtues of Ru and may be even better than Ru in some ways: they have weaker interaction with water vapor, more weakly-bonded oxide than Ru, and are easily reduced by gaseous hydrogen or CO, with gentle heating. Rh and Pd are effective catalysts for oxidation of CO ($2CO + O_2 \rightarrow 2 CO_2$) and for hydrogenation of C and CO to CH_4. None of the three metals Ru, Rh, Pd are reported to form stable carbides.[2 - Footnote]

***Radiation damage*:**

Radiation damage by EUV generally does not occur for elemental metal films; the lifetimes of electronic excitations are too short for electronic energy to be converted to atom motion. Of course, it is well documented that EUV causes dissociation of adsorbed molecules and can accelerate oxidation and carbon deposition on the surfaces. Dissociation of molecules, or desorption of neutral or ionic products may occur during irradiation; these processes include electron-stimulated desorption (ESD), photon-stimulated desorption (PSD), and radiation-stimulated dissociation and reaction.[84,85] In

[2] The EUV reflectivity performance of Ir when deposited on the test multilayer stack for the reflectivity calculations shown in this work ($\Delta R = 1.74\%$ for a 2nm capping layer film) eliminate Ir as a serious contender.

these radiation-induced processes, an atom or molecule at a surface is electronically excited via core or valence excitations to a repulsive state. Desorption occurs if the repulsive state is sufficiently long-lived for the species to gain enough kinetic energy to exit the surface (kinetic energies of desorbed atoms and ions are often a few eV). Alternatively, a surface reaction (e.g., oxidation, or carbon deposition) may occur if enough energetic, reactive product atoms are directed toward (rather than away from) the surface.

Low energy electrons play an important role in radiation-induced processes at surfaces. For all forms of ionizing radiation incident on solids (including electrons, energetic photons, and even ions) the dominant product is a cascade of low energy secondaries.[86,87] The primary mechanism by which 13.5 nm (93 eV) photons are absorbed in a substrate involves valence and shallow core photoexcitations of electrons in surface and sub-surface atoms. A fraction of these electrons propagate to the surface and escape as secondary electrons; secondary electrons induce electronic excitations in the surface layer that cause dissociation and reaction of surface molecules.

In addition to radiation-induced reactions of adsorbed molecules, another phenomenon should be noted: PSD and ESD can cause removal of O from oxides and oxygen-covered metals, forming O-vacancies at the surface. This PSD process is initiated by direct photo-creation of holes in shallow core levels (e.g., Ti 3p at a binding energy ~35 eV for TiO_2). An interatomic Auger-decay process can lead to a "Coulomb explosion" and ejection of

O^+ ions.[88] The probability (cross section) depends on various factors, including the photoionization probability for 13.5 nm photons.

3.2.3 Binary compounds with [R (Si) - Rmax] or [R(Mo) - R max] < 2.0

The list of possible compounds tabulated in Table 2 with suitable optical properties (mainly for capping top Si layers on the multilayer stack) includes:

LiH, LiOH

Be_4C, BeO, BN, various hydrocarbon films, including fluorocarbons (teflon) and chlorinated hydrocarbons

SiC, Si_3N_4, SiO_2

CaF_2, CdS, GaP

TiN, TiO_2, Cr_2O_3, MnO, MnO_2, $CoSi_2$, Co_2O_3, Co_3O_4

ZrO_2, Y_2O_3, MoO_2, MoO_3, $MoSi_2$, $RuSi_2$, RuO_2, RuO_4

UO_2

Certain of these materials are clearly unsuitable. These include the alkali hydride and hydroxide, LiH and LiOH, as well as SiO_2 and Mo oxides (MoO_2, MoO_3), as discussed above. Such species as GaP, InN, and In_2O_3 are unsuitable because of defectivity issues (see Appendix E). CaF_2, CdS, GaP suffer from various problems including radiation damage.

Other *inappropriate* materials are hydrocarbons, and halogenated hydrocarbons, including freon. Films of these materials are highly sensitive to radiation damage induced by EUV.[89] The main culprits are the low-energy secondary electrons released from the substrate exposed to EUV, with energies in the range 0 eV to ~ 20eV. In general, covalently bonded hydrocarbons are readily dissociated by low energy electrons; e.g., the threshold energies for breaking of C-H bonds in alkane chains are ~ 5eV, with a maximum cross section (probability of bond-breaking) at ~ 10eV.[90] For species containing C-Cl and C-F bonds, the threshold energies for bond-breaking by low energy secondary electrons are even lower, in the range 0 - 5eV; the maximum cross sections can be quite high, > 10^{-16} cm^2. The dissociation mechanism at low energies involves dissociative electron attachment (DEA); a low energy electron is captured and excites the molecule vibrationally or electronically in a transient negative ion (TNI) state. Dissociation of the TNI occurs via elimination of an anion.[86]

There are *potentially appropriate* materials on the list above. It is interesting to note that there are several pairs of materials (element and compound, e. g., Ti and TiO_2) which have favorable optical properties (high reflectivities) for 2 nm films on Si top layers. Other such pairs (and groupings of 3 and 4) of elements and compounds for which optical properties are favorable include

Be, BeO

Si, SiO_2, Si_3N_4, SiC

Ti, TiO_2, TiN

Zr, ZrO_2

Ru, RuO_2, Ru_2Si_3

U and UO_2

The implication is interesting: even if an as-deposited metal film subsequently oxidizes, there may be circumstances for which there is little degradation of reflectivity. There may be other such materials groupings, but optical data for the compounds are unavailable. It is certainly possible that if the metal and the oxide have favorable optical properties, the carbides and nitrides will also have favorable optical properties—certainly differences between the surface chemistry of the carbide and nitride would in many cases be larger than the differences in density/ optical performance. One could adopt the viewpoint that materials whose reflectivities are known to be favorable for both metal and oxide (or nitride, or carbide) might be especially good candidates for consideration. Of course, the surface chemistry and radiation stability must be considered. A good introduction to oxide surface chemistry is by Henrich and Cox.[91]

For the pairs Ti, Zr, Ru and their oxides, only Ru has an oxide with a relatively low heat of formation, which means that it can be reduced chemically to the metal (e.g., exposure to high pressure H_2 while gently heating, or exposure to H-atoms; CO will partially reduce RuO_2).[92,**Error! Bookmark not defined.**] So, one can deposit a metallic Ru film that develops a very thin oxygen/oxide layer that (in principle) can be removed in vacuum (Figures 4 and 5). At least, it does not grow readily in background gas alone, and most of the 2 nm film remains metallic even after air exposure. The others (Ti, Zr) may be deposited as metals but they can form very stable oxide films that cannot be reduced by

high pressure hydrogen, and it is unlikely that atomic H will do much to them (other than form surface hydroxyl). Thin films of metallic Ti and Zr will slowly and (almost) irreversibly convert to oxide, or oxycarbide, depending on the ambient gas composition and the effects of radiation-induced surface chemistry.

TiO_2 has attracted much interest recently in the EUV community, and shows promise as a capping layer material; an extensive summary of its surface chemistry and physics is given by Diebold.[93] One virtue of TiO_2 is that much is known about its surface chemistry - it is safe to say that surfaces of TiO_2 are more widely studied by surface scientists than surfaces of any other oxide. Photon stimulated desorption of O[94] is a potential problem with TiO_2 and other oxides; see discussion below.

Some oxides such as RuO_2, Co_3O_4, V_2O_5, MnO_2, (and others) are active as CO oxidation catalysts; this reaction can be a pathway to creation of O-vacancies. The mechanism is believed to involve CO adsorption at the metal cation site; the adsorbed CO reacts with neighboring lattice O to make CO_2, which desorbs from the surface. The O-vacancy is then filled by dissociation of an incoming O_2 molecule, and the process starts over again. In the absence of O_2, CO alone can partially reduce the oxide, at least in the top layer. Also, impurities in the background gases (hydrocarbons, H_2O) can poison the surface and inhibit CO oxidation at low T. The surface composition of such materials could be changing constantly under EUV exposure conditions as O-vacancies are created; see "radiation damage" paragraphs below. It is documented that x-ray exposure accelerates CO oxidation on V_2O_5 catalysts.[95]

Silicides, Nitrides, Carbides

Nitrides react with oxygen to form oxynitrides. For example, it is thermodynamically favorable for TiN to be oxidized.[96] The literature on surface chemistry of carbides, nitrides, oxynitrides, etc. is sparse, and it will be difficult to draw valid general conclusions about these materials. There is literature on the surface chemistry of a few carbides.[97]

One carbide for which there is copious literature is SiC, and this illustrates the challenge of working with such a material in the form of thin-film capping layers. SiC exists in various crystallographic phases (including cubic, rhombohedric and hexagonal) with more than 170 polytypes![98] What form(s) of SiC would be produced in sputter-deposited films below 200ºC depends critically on growth conditions.[99] Because of the interest in SiC as a material for high temperature semiconductor devices, there have been many studies of hexagonal 6H-SiC and 4H-SiC polytypes. While the reactivity of SiC depends on polytype and surface termination (C-layer or Si- layer), it is clear that SiC is highly reactive toward low exposures of O_2 in vacuum, with SiO_2 as the dominant oxidation product.

There is experimental evidence that a thin layer of SiO_2 (or SiO-C) forms on top of SiC layer after exposure to the air. It also appears that the reactivity and thickness of SiO_2 depends on the amount of excess Si in the top layer(s). If there is a limiting SiO_2

thickness of a few monolayers, that may serve as a passivation layer, this would make SiC more interesting as a capping layer candidate, though more work must be done to assess the utility of SiC thin films as a capping layer. The same applies for $MoSi_2$, which is widely used as a film to passivate Mo and other metals against rapid oxidation. LLNL observation of possible subsurface oxygen diffusion in irradiated SiC, however, makes the use of this capping layer less attractive. At LLNL, on *as-deposited* SiC thin film exposed to the air three peaks in the XPS spectrum were measured, with energies of 102.8, 99.9, and 98.8 eV. These correspond to oxidized Si, SiC, and elemental Si, respectively. The elemental Si is from the underlying multilayer, while the SiC and SiO_2 result from a partially oxidized SiC capping layer. After EUV exposure in the presence of water vapor, the exposed area spectrum exhibits a predominant peak at 103.1 eV, which is close to the SiO_2 binding energy (103.3 eV). The minor peak at 97.4 eV (7 at. %) is at a very low binding energy and possibly corresponds to Si in interstitial positions or surface defects. Thus EUV irradiation might have removed SiC in the exposed area. In addition, the lack of an elemental Si peak in the exposed area spectrum indicates the underlying Si layer also has been oxidized. Because of numerous polymorphs of crystalline SiC it is also difficult to find well characterized, good quality crystals and apply the knowledge to the low-temperature amorphous thin film SiC.

Radiation damage at the surfaces of oxides

Radiation damage by EUV photons is a potential serious problem for oxygen-covered metals and oxide surfaces: photon-stimulated desorption (PSD) and electron -stimulated

desorption (ESD) can remove O from the surface. Why should we be concerned about ESD and PSD of oxides? The main radiation damage mechanism for O-covered surfaces and oxides is the formation of O vacancies, i.e., creation of surface defects. Background gas molecules (water, hydrocarbons, etc.) are generally more chemically reactive with defects than with stoichiometric surfaces, so the surface chemistry is altered and generally accelerated.

Here's how it happens. It has been known for years that bombardment of oxide surfaces with energetic electrons and extreme UV photons leads to desorption of O^+ ions, as well as neutral O by ESD and PSD. Since oxygen in oxides is electronegative with formal charge O^{-2}, there must be charge transfer to create neutral O and O^+. An Auger-stimulated desorption model, originally proposed by Knotek,[100,101] explains these observations. This mechanism involves the excitation of core electron levels followed by an Auger decay to repulsive electronic configurations that cause desorption.

The oxides for which the desorption yields are highest are the so-called maximal valency oxides. Maximal valency means that the cation is nominally ionized down to the rare gas electronic configuration (e.g., K^+, Ca^{2+}, Sc^{3+}, Ti^{4+}, V^{5+}… in K_2O, CaO, Sc_2O_3, TiO_2, V_2O_5,..).[100] The highest occupied level (in a formal chemical sense) is its highest core level, with binding energy > 25 eV or so. Of course, there is always some degree of covalency in such oxides and the actual charges on anions and cations are not as large as indicated, but to a first approximation, this description is a useful construct. In fact, many maximal-valency oxides (e.g., TiO_2, V_2O_5, ZrO_2, Ta_2O_5, MoO_3, WO_3, CeO_2, Er_2O_3,….)

have high cross sections for radiation-stimulated desorption of oxygen, initiated by creation of holes in shallow core levels.

TiO_2 is a prototypical example. Consider what happens when photoionization of the Ti 3p level occurs to form a core hole (vacancy); the Ti 3p binding energy is ~35 eV for TiO_2. Because of a deficiency of higher lying electrons on the Ti cation, a valence electron from the O 2p level falls into the Ti core hole, initiating an interatomic Auger decay process. Energy is conserved by ejection of one or two more 2p electrons from the O species; thus the charge on the O anion changes from O^{2-} to O^+. The presence of O^+ near Ti^{4+} leads to a "Coulomb explosion" and ejection of O^+ ions.[102] Neutral OH can also desorb from TiO_2, due to a bonding-antibonding excitation with a threshold of ~ 11.5 eV.[103] Recent work demonstrates that the photon-stimulated desorption mechanism for TiO_2 is more complicated than indicated above, but the observation that core hole excitations initiate desorption of O is confirmed.[104]

Whereas PSD of O^+ from TiO_2 and many of the other maximal valency oxides by EUV photons is well known, PSD and ESD of O is observed even for non-maximal valency oxides (CrO_2, NiO) via the Auger stimulated desorption mechanism[105]; the key factor is the localization of the repulsive electronic excitation. Note that the relevant excitations involve shallow core holes with binding energies > 25 eV (thus, they can be excited by the primary photon (rather than by low energy secondaries, which induce dissociation of adsorbed molecules). Although RuO_2 is not a maximal valency oxide, we have found

recently that low energy electrons (25eV to 100eV) cause desorption of O^+, O^- and O from O-covered Ru.[106]

We summarize as indicated above: The main radiation damage mechanism for O-covered surfaces and oxides is the formation of O vacancies, i.e., creation of surface defects. Background gas molecules (water, hydrocarbons, etc.) are generally more chemically reactive with defects than with stoichiometric surfaces, so the surface chemistry is altered and generally accelerated. This must be considered in choosing a capping layer for a specific EUV environment (gas composition, partial pressures, radiation load).

Caveat: Additional Issues that should be addressed

The previous discussion does not take into account the following, which may impact capping layer performance from a "reactivity" point of view. When considering the growth mode of elemental materials (metals) on multilayers, it is important to understand whether the growth proceeds layer-by-layer or a form of cluster growth.[107] It is critical to also understand how the film morphology is affected by subsequent reaction with background gases. Ease of vacancy formation, which plays a key role in capping layer degradation, will depend on radiation and background gases. Further work needs to be done to elucidate mitigation processes for the classes of materials under consideration -- including role of H atoms.[108] These are all issues that should be considered in capping layer development, that are currently not fully understood.

3.2.4 Ternary compounds

Certain epitaxial perovskite films containing a rare earth, specifically $SrTiO_3$, $BaTiO_3$ and $DyScO_3$, are relatively robust when exposed to air. The stabilizing effect of the TiO_2 (or ScO_2) reduces the reactivity of the RE or alkaline earth components. Of course pure SrO, BaO, etc. are reactive with H_2O and CO_2 to make hydroxides and carbonates. So if one can find a way to make epitaxial films over a 100-200 mm diameter mirror, these may be worth a look. Etching of $BaTiO_3$ in buffered solution leads to removal of the BaO layer and termination of the surface by TiO_2.

3.2.5 Best Materials Choices…

Based on the above, and with little knowledge of film growth considerations, here are the "best bets" from a "surface chemistry" point of view. If the following materials can be deposited on Si capping layers and remain stoichiometric, smooth and continuous, and if pinholes and grain boundaries are minimal, they may be worth considering for further development of a research and characterization strategy.

Elemental materials: **Ru, Rh** (Figure 6)

Compounds: **TiO_2, ZrO_2**

In the following three sections, we address other issues concerning these four materials, as well as related mateials. The topics include environmental and health safety concerns,

thin film fabrication challenges, and the effects of defects and nanostructure on diffusion of contaminating species.

4. Environmental Health and Safety Concerns

Beryllium (Be) and BeO, despite their favorable performance with respect to our first two criterion, should be eliminated because the exposure to the beryllium metal dust and fumes can cause major lung damage and beryllium salts are very toxic.[109] Compounds containing beryllium are very poisonous. Ruthenium compounds present similar problems, especially the volatile compound RuO_4.

5. Thin Film Fabrication and Related Issues

Most commonly used techniques to fabricate EUV multilayer films are magnetron or ion beam sputtering, and electron beam evaporation with ion beam smoothing, though other modes of film deposition, though not yet demonstrated, may be possible (e.g., atomic layer deposition (ALD), molecular beam epitaxy (MBE), modified chemical vapor deposition (CVD) arrangements). The highest reflectivity multilayer coatings of 70% (Figure 7) were achieved with interface engineered multilayers fabricated with the magnetron sputtering technique.[9,110] In this section we will leverage LLNL knowledge of thin film development and magnetron sputtering to determine whether amorphous films of the best capping layer candidates, Ru, Rh, TiO_2, and ZrO_2, can indeed be deposited.

Work on ruthenium, which extends projection optics lifetime as compared to Si-capped multilayers, originated at LLNL as part of the VNL project.[9,10,11] Further work on ruthenium capping layers, focused on establishing the baseline structural, optical and surface properties was supported by SEMATECH as part of LITH160 project.[111] These Ru-capped Mo/Si-based EUVL multilayers are also known as Multilayer 1 in EUVL community. Differently prepared Ru capping layers (change in voltage/current, change in sputtering gas, and a variation of material) were tested for their oxidation and thermal stability. The best performing Ru-capping layer structure was prepared using Ar sputtering gas and metallic Ru target. The microstructure of this capping layer was analyzed in detail with transmission electron microscopy (TEM).[12] Compared to other Ru capping layers preparations it is the only one that shows grains with preferential orientation. Ruthenium in this capping layer preparation is polycrystalline with an average grain size of ~3.5 nm and has a preferential growth orientation with Ru(0001) crystal planes parallel to the specimen surface (Figure 8). Based on limited TEM data it appears that the Ru capping layers of other preparations have smaller, randomly oriented and mostly oxidized grains. Based on our experience it would require a major effort to grow Ru on the top of the multilayer in a desired orientation for such thin layers, but it is possible.

As part of the SEMATECH funded project LLNL also fabricated and tested five more capping layer candidates, which included Pd, PdAu, SiC, YSZ (Y_2O_3 stabilized ZrO_2) and $MoSi_2$.[112] Although none of these materials outperformed Ru we learned much about different degradation mechanisms. This feedback was very useful for improving the

properties of these and other capping layer materials. The reflectivity of the capped multilayers ranged from 62.6% to 67.4%. The samples listed according to their reflectivity values from the highest to the lowest are SiC, YSZ, $MoSi_2$, PdAu and Pd. These values are consistent with the ranking based on calculated reflectivities. For example, a 3 nm thick Pd-capped multilayer has 5.8% lower reflectivity than Si-capped multilayer. A PdAu-capped multilayer should have even lower reflectivity than a Pd-capped multilayer if we only consider optical constants. However, as discussed below, in addition to the optical properties the reflectivity and the lifetime are also highly dependent on interdiffusion, incomplete coverage and surface roughness.

For example, Pd and PdAu capping layers both show island growth formation with associated surface roughness and incomplete coverage. In addition, we detect Pd and Au in the layers below the capping layer, suggesting diffusion of these elements into the multilayer. Insertion of a diffusion barrier (such as C) between Si and Pd (PdAu) limited the diffusion into the multilayer and increased the reflectivity by **20%**. Even though noble metals are impervious to oxidation in bulk form substantial development is required to overcome island growth and to limit diffusion into the bulk of the multilayer. While thicker Pd (PdAu) layers will completely cover the surface, such a thick layer (>4 nm) leads to unacceptably low reflectivity. Another noble metal, Rh, might be a good candidate for a capping layer. Based on calculated reflectivity it is a better choice than Pd although not as good as Ru. Some work done on Rh/C multilayers shows that Rh, from the point of fabrication, is very similar to Ru[113]. This same work also demonstrated that

Rh and C form relatively sharp interfaces. Hence, carbon could be used as a diffusion barrier between Si and Rh, if necessary.

SiC deposited for a SEMATECH-funded project was remarkably smooth and most likely amorphous. However, even in as-deposited state the SiC surface shows presence of Si-oxide and elemental carbon. No data exist on the stoichiometry or density of the SiC that was used as a capping layer and was deposited with rf-sputtering technique. However, the SiC sputtered via dc-magnetron, which was used in high temperature stability multilayers,[114] was studied in more detail with RBS, XPS and TEM techniques. It was determined that SiC from a conductive target is amorphous in its as-deposited state and has correct stoichiometric composition within 2 at. % accuracy. Mo/SiC multilayers developed for high temperature operation were capped with SiC and show remarkable reflectance stability for temperatures up to 400°C, though no lifetime data from EUV exposures are available for these layers.

$MoSi_2$ is an alloy that forms naturally on Mo/Si interfaces during the multilayer growth and its growth is accelerated at higher temperatures. For LITH160 SEMATECH-funded project $MoSi_2$ was sputtered from an alloy target. No stoichiometry, density or microstructure data exist about the deposited $MoSi_2$ films. Later analysis of the deposited films revealed that the alloy target was carbon contaminated and that the stoichiometry of the deposited film was $MoSi_{1.3}$ instead of $MoSi_2$. The Mo-silicide film is amorphous in as-deposited state and very smooth. For a later project a new, better quality sputtering target was purchased. Optical constant measurements of $MoSi_2$ films revealed large

discrepancy between the calculated optical constants[115] and our experimentally determined ones.[116] We believe that the calculated optical constants overestimate the reflectivity of $MoSi_2$-capped multilayers in EUV range.

YSZ was the only capping layer material that did not change when exposed to the EUV light in the presence of water vapor. Even though there is no microstructural data on our YSZ capping layer this material is very smooth and most likely amorphous or consists of very fine crystallites. YSZ is thermally stable and its microstructure and properties are highly dependent on its exact composition (percentage of Y_2O_3 in ZrO_2). The O diffusion rate through our YSZ alloy was very high. Even though the YSZ layer remained unchanged the Si and Mo layers underneath were oxidized. That led to the highest reflectivity loss among the capping layer materials that were tested in this project. Note that though Yittria is used to stabilize ZrO2 in its high temperature phase to enhance diffusion of oxygen ions for sensor applications, this enhancement is not general and is only effective for a narrow range of compositions.

TiO_2 is one of compounds that has favorable optical and surface reactivity properties. A 2 nm thick TiO_2 capping layer reduces the reflectivity by only 0.8% as compared to Si-capped multilayer. This material belongs to the class of semiconductors with a relatively wide band gap. Being exposed to the light of the energy corresponding to its band gap, charge carriers, such as electrons and holes, are produced and oxidation-reduction reactions on the TiO_2 surface occur. TiO_2 thin film has strong oxidizing power and high photocatalytic activity for hydrocarbon oxidation[117] and is therefore of interest also as a

potential self cleaning capping layer. Previous work[118] on TiO_2 indicates that the use of reactive magnetron sputtering provides more benefit to control the structure, composition and properties of TiO_2 films than other methods, such as PECVD, thermal oxidation of metal, sol-gel, etc. When fabricating titanium oxide films by magnetron-sputtering with titanium oxide targets, parameters such as Ar/O_2 ratio, deposition power and substrate temperature were found to strongly influence the formation of titanium oxide films. In our studies TiO_2 was prepared in three different ways: (a) depositing metallic Ti layer and then oxidizing it with pure O_2, (b) rf-sputtering of TiO_2 target and (c) reactive rf sputtering of TiO_2 target with $Ar:O_2$ sputtering gas mixture. The later method produced >66% reflectivity multilayers and the preliminary exposure results with H_2O vapor indicate about 10x longer lifetime as compared to Ru-capped multilayers.[119] The TiO_2 capping layer prepared with reactive rf-sputtering is amorphous and completely covers the multilayers as demonstrated with TEM studies. TiO_2 layer also forms a sharp interface with Si so no diffusion barrier is necessary. However, XPS and STEM analysis indicate Ar gas incorporation in TiO_2 capping layer and the stoichiometry of $TiO_{2.4}$. Further work on optimization of deposition process, such as $Ar:O_2$ gas mixture and energy of the incoming ions, is required to improve the performance of this capping layer material.

Based on this experience it is our opinion that with some additional development work amorphous layers of Ru, Rh, TiO_2, and ZrO_2 could be deposited in the strict deposition parameter space dictated by EUV optics capping layer requirements.

6. Vacancy Management: Defects, Diffusion, and Nanostructure

It is difficult to divorce thin film defect management issues from surface chemistry performance for potential capping layer materials given our knowledge that the background gas molecules present in the unbakeable projection optics chamber will be more chemically reactive with defective than with stoichiometric surfaces. Though a dire scenario, it is essentially an idealized and optimistic view that confines contamination to the surface of an infinitely thick optics capping layer, assuming no penetration of contaminating species into the layer beneath. Experience has taught us to view the capping layer otherwise; contamination for EUV optics is exacerbated by the fact that diffusion of oxygen through the capping layer has been shown to be a serious degradation mechanism, where such bulk diffusion can even lead to oxidation of the underlying silicon layer and catastrophic failure of the optic.[120] In what may appear to be a spate of pessimism, we must also point out that "bulk" diffusion is hardly an accurate descriptor, given that our previous calculations in Section 3.1 have demonstrated that optics capping layer films can only be two or three nanometers thick under the most favorable circumstances. It is not only critical to consider whether a smooth and continuous 2 nm thick film of a candidate material can be fabricated, but we must also concern ourselves with engineering the nanostructure of the capping layer to minimize diffusion of oxygen through the layer.

There are additional issues to consider when engineering nanoscale properties of EUV optics capping layers. Capping layer design must also take into account that (1) diffusion behavior for very thick films will be quite different from behavior for layers several nanometers thick and that (2) most formalism describing diffusion behavior exclusively considers temperature-driven mechanisms, where the relationship between surface diffusion of contaminants, electron- and photon-mediated processes at the sample surface and subsequent diffusion behavior in the "bulk" is largely unknown. Given the additional challenge that there are large gaps in the literature concerning diffusion behavior of relatively thick films of relevant materials (of sufficiently similar microstructure to allow comparison), it is not yet possible to make iron-clad judgments about the diffusion performance of ZrO_2, TiO_2, Ru, and Rh relative to one another in such a way that would allow us to further narrow our choice of materials. We can make general commentary, however, about diffusion behavior in broad material classes. Enough information exists for us to elucidate outstanding questions that both provide general guidelines about how to evaluate our collection of contending capping layer materials and indicate that it may be possible to transcend conventional thinking about diffusion in EUV capping layer materials to create "diffusion-engineered" thin films.

After observation of EUV optics lifetime failures due to oxygen diffusion through the capping layer, it became generally accepted in the EUVL community that capping layers should be amorphous to prevent diffusion.[121] This might be true, but it has not been adequately demonstrated. Granted, it is well-known that diffusion can proceed more rapidly along grain boundaries and dislocations than through the bulk lattice. Short-

circuit diffusion pathways are typically preferred to bulk transport mechanisms by diffusing species at low temperatures, for smaller grain sizes, and in cases where there is a low concentration of lattice defects.[122] In metals, it is generally accepted that atomic jump frequencies in planar defects (which are only several atoms thick) are literally a million times greater than jump frequencies in the regular crystal lattice.[123] Atkinson[122] also maintains that diffusion occurs preferentially along grain boundaries and other structural defects because there is more disorder in the arrangement of atoms in these regions than in the ordered bulk crystal lattice. However, under certain conditions if the bulk is highly disordered, grain boundaries and dislocations will actually act as barriers to diffusion, but these conditions are not well understood.

TiO_2 and ZrO_2 are two of the surviving candidates (in addition to Ru and Rh) for our capping layer selection; consistent with the previous logic grain boundaries are actually observed (and confirmed by molecular dynamics calculations) as a source of oxygen diffusion resistance in polycrystalline zirconia ceramics.[124] Perhaps in these cases the lattice is sufficiently disordered to provide preferential diffusion pathways; indeed, we know that some metal oxides, for example, are plagued by non-uniform grain size, porosity, second phase distribution issues, impurity segregation and grain-grain disorientation[125] that can offer alternative diffusion pathways and render results from radioactive tracer diffusion studies difficult to interpret. Recent research on nanocrystalline materials claims that the volume diffusivity of oxygen in undoped monoclinic ZrO_2 will be (in comparison with the melting temperature) much higher than in the other transition metal oxides, but far lower than if the material is stabilized with

impurities to maximize oxygen diffusion.[126] However, it is difficult to generalize results from one sample type to another, as microstructure is critical for understanding diffusion behavior. Indeed, nanocrystalline TiO_2 has much faster oxygen diffusion than crystalline TiO_2, for example, but the exact dependence on grain size is not generally understood:[127] In ZrO_2, grain boundary conductivity is thought to decrease with decreasing grain size, down to ~0.36 microns[128] but a similar enhancement of oxygen diffusion is predicted for even smaller grains.[129] One conclusion to draw is that thorough analytical characterization of a candidate capping layer to understand often complex structural defectivity in these disordered materials will be critical for understanding failure mechanisms and optimizing material design. Given the influence of sample microstructure on isotopic tracer diffusion experiments, such experiments should be performed on well-characterized actual capping layer materials, not bulk samples, in order to allow a proper comparison between candidate capping layer materials.

Though metal oxides can be sufficiently disordered such that multiple diffusion mechanisms compete for supremacy, it should be noted that when comparing these materials to other candidates that they are considered superior "diffusers" of oxygen. As such, one would expect that their diffusion behavior would be less optimal than for Ru or Rh of *identical* nanostructure. (In reality, it would be nearly impossible to produce such comparative samples, meaning that further investigation to determine optimized nanostructure for Pt group metals is needed before a proper comparison could be made). Zirconia, stabilized in its high temperature cubic form by the addition of 8 mol% Y_2O_3, is a solid state oxide ion conducting electrolyte material of choice, used for oxygen sensors,

oxygen pumps, and solid oxide fuel cells.[130] Unstabilized, as we have discussed, oxygen transport is dramatically reduced, though still higher than the other transition metal oxides for nanocrystalline material.[131] This observation would provide some guidance for comparing TiO_2 vs. ZrO_2 (TiO_2 would be a better choice) if, again, the microstructure results were generalizable to other structures and if identical structures of both materials could be fabricated. It is not possible to make further judgment about diffusion performance of our capping layer candidates without additional data. We provide below, however, some key references to allow the reader to judge for him or herself.

For additional information on diffusion-related phenomena, there are some key references that are very informative such as a seminal work on grain boundary diffusion in thin films by Gupta et al.[132] and other excellent treatments of the same topic in metals and metal oxides.[133,134,135] Diffusion in disordered media has been discussed by Havlin et al.,[136] and percolation theory treatments of diffusion in amorphous materials are available as well, though these publications make it clear that additional work is needed, from an experimental point of view, to evaluate potential capping layer materials.[137,138,139]

7. Thermal Stability

Not surprising ceramic materials such as SiC, YSZ, and $MoSi_2$ show very good thermal stability. Multilayers capped with these materials show little loss in reflectivity when exposed to 200°C, unlike Pd- and PdAu- and Ru-capped multilayers, which show reflectivity loss between 1.5% and 3.5%. The thermal stability of TiO_2 and ZrO_2 is not known; though it is well known that very high temperatures cause phase changes in metal

oxides, which can be stabilized by the presence of impurities.[140] These temperatures are typically far higher than those experienced in an EUVL projection optics chamber environment. Additional experiments would be necessary before ranking the contending capping layer materials (ZrO_2, TiO_2, Ru and Rh) in terms of their thermal stability.

8. Summary

High volume manufacturing tools for Extreme Ultraviolet Lithography (EUVL) require optics with 30,000 light-on hours of lifetime. The optics used to reflect and focus 13.5 nm (92 eV) EUV radiation are Si/Mo multilayer mirrors (MLMs) which function in ~10^{-7} Torr vacuum of EUVL exposure tools. Their lifetimes can be extended by coating the multilayers with thin (~ 2nm) capping layer films that reduce build-up of contamination (mostly oxides, carbon films). Despite recent progress the optics lifetimes still fall short by nearly two orders of magnitude. In this paper we evaluate most of the solid phase elements in the periodic table and their material combinations as possible capping layer candidates. Our design criteria select only materials that do not reduce reflectivity below a level that would render it unsuitable for lithographic purposes, where the film is continuous and smooth over only several nanometers of thickness and where the material can be deposited at sufficiently low temperature (<200°C) to avoid intermixing with the underlying multilayer stack. In addition, we take into account nanoscale capping layer properties and complex surface chemistry. Ideally, the surface of the capping layer would inhibit adsorption and reaction of background gases, and induce recombination of impurity atoms to form species that could be desorbed thermally or by electron- or photon-stimulated desorption processes associated with the incident EUV flux. Based on

these criteria and available experimental data we down-select the most promising candidates. These include Ru, Rh, TiO_2 and ZrO_2 assuming that these can be deposited as amorphous films. Additional candidates Hf, HfO_2 and V, V_2O_5 are suggested based on their surface reactivity, film growth, thermal stability, and diffusion-related behavior. However, additional work is necessary to verify their optical performance.

Acknowledgements

Work by S.B. was performed under the auspices of the U.S. Department of Energy by the Lawrence Livermore National Laboratory under Contract No. W-7405-ENG-48. This project was funded by SEMATECH under Project LITH 160.

Figure Captions

Figure 1: TEM cross section of a Mo/Si multilayer showing crystalline Mo (dark layers) and amorphous Si (light layers). The right image shows the top part of the multilayer, including the capping layer.

Figure 2: Schematic of an EUVL prototype Engineering Test Stand system, designed, fabricated and tested by Sandia National Laboratories, Lawrence Livermore National Laboratory and Lawrence Berkeley National Laboratory and funded by the Extreme Ultraviolet Limited Liability Company. The mirrors labeled C1-C4 are condenser optic mirrors and M1-M4 are projection optics mirrors. The focus of this paper is the lifetime issue associated with the projection optics mirrors.

Figure 3: All non-shaded elements in the periodic table have good optical properties.

Figure 4: Figure 8: Schematic of atomic-hydrogen cleaning apparatus (Figure from [141]).

Figure 5: Auger Electron Spectroscopy depth profiles for Ru-capped multilayer mirror: (a) initial (as-deposited), (b) after ECR O2 plasma oxidation and (c) after 20-min atomic hydrogen treatment (left column). Righ column plots show X-ray photoelectron spectra of Ru $3d_{3/2}$ and $3d_{5/2}$ peaks for Ru-capped multilayer mirror: (a) initial (as-deposited), (b) after ECR O2 plasma oxidation and (c) after 5-min atomic hydrogen treatment (Figure from **Error! Bookmark not defined.**).

Figure 6: Only two pure elements pass all the screening tests: Ru and Rh.

Figure 7: Performance of a 70% reflectivity EUV mirror (5deg off normal) with 50 bilayers.

Figure 8: TEM cross section of a Mo/Si multilayer showing crystalline Mo (dark layers) and amorphous Si (light layers). The right image shows the top part of the multilayer, including the capping layer.

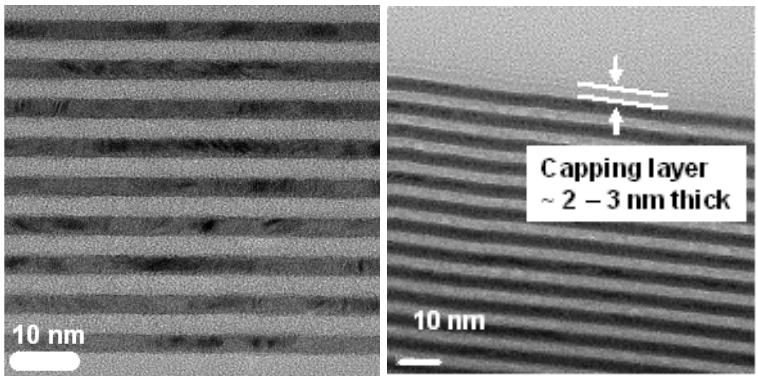

Figure 1

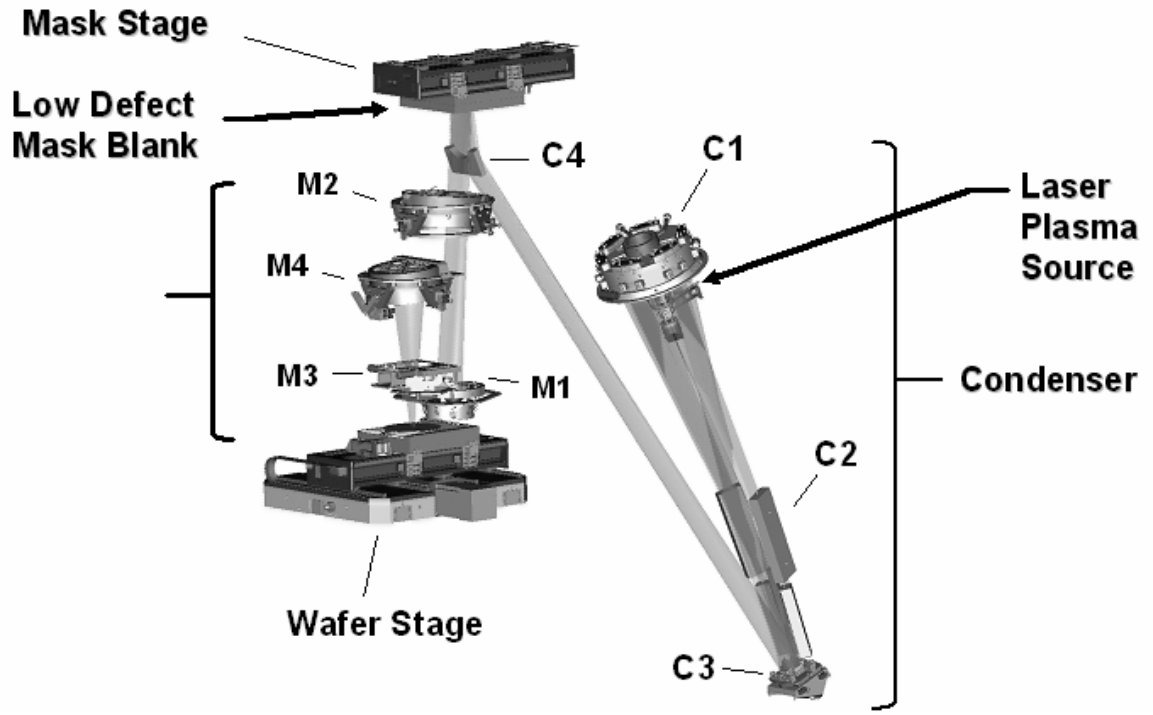
Mask Stage
Low Defect
Mask Blank
C4
C1
M2
Laser
Plasma
Source
M4
M3
M1
Condenser
C2
Wafer Stage
C3

Figure 2

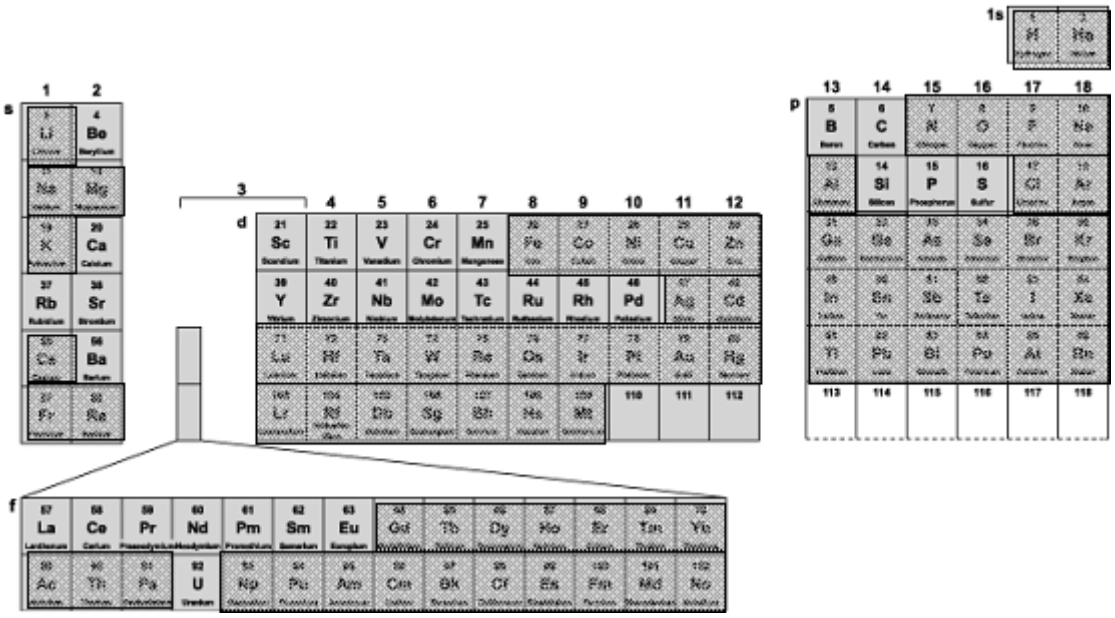

Figure 3

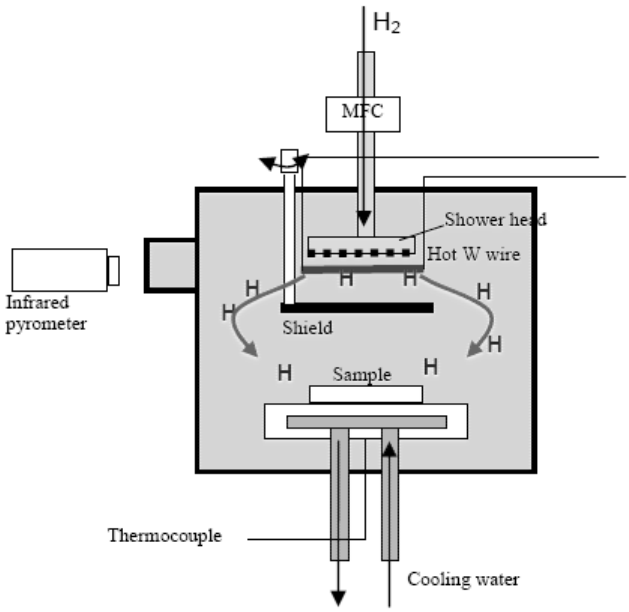
H2
MFC
Shower head
Hot W wire
Infrared
pyrometer
H
H
H
H
H
H
Shield
H
Sample
H
Thermocouple
Cooling water

Figure 4

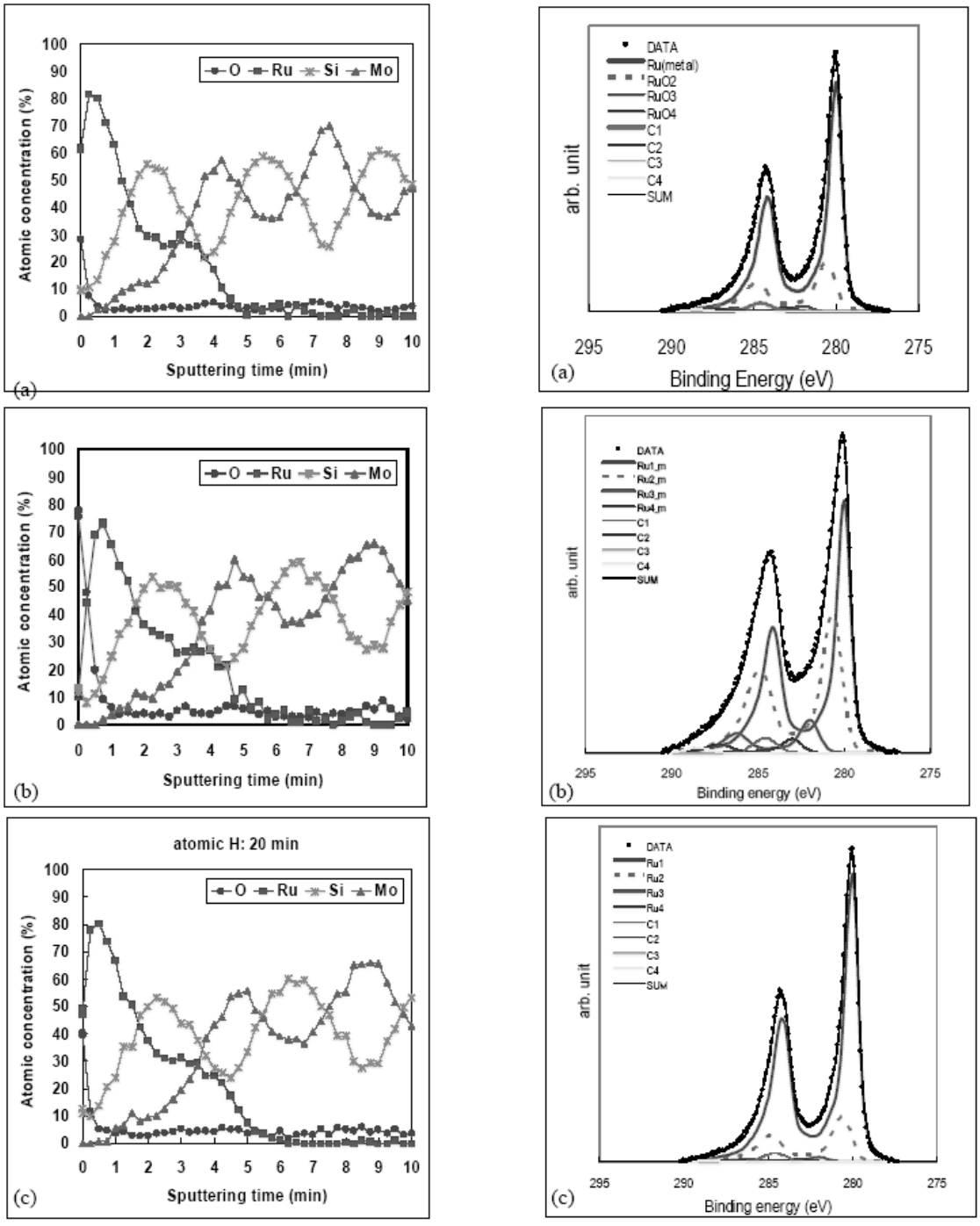
O
Ru
Si
Mo
Atomic concentration (%)
Sputtering time (min)
(a)
(b)
(c)
atomic H: 20 min
DATA
Ru(metal)
RuO2
RuO3
RuO4
C1
C2
C3
C4
SUM
arb. unit
Binding Energy (eV)
Binding energy (eV)
Ru1_m
Ru2_m
Ru3_m
Ru4_m
Ru1
Ru2
Ru3
Ru4

Figure 5

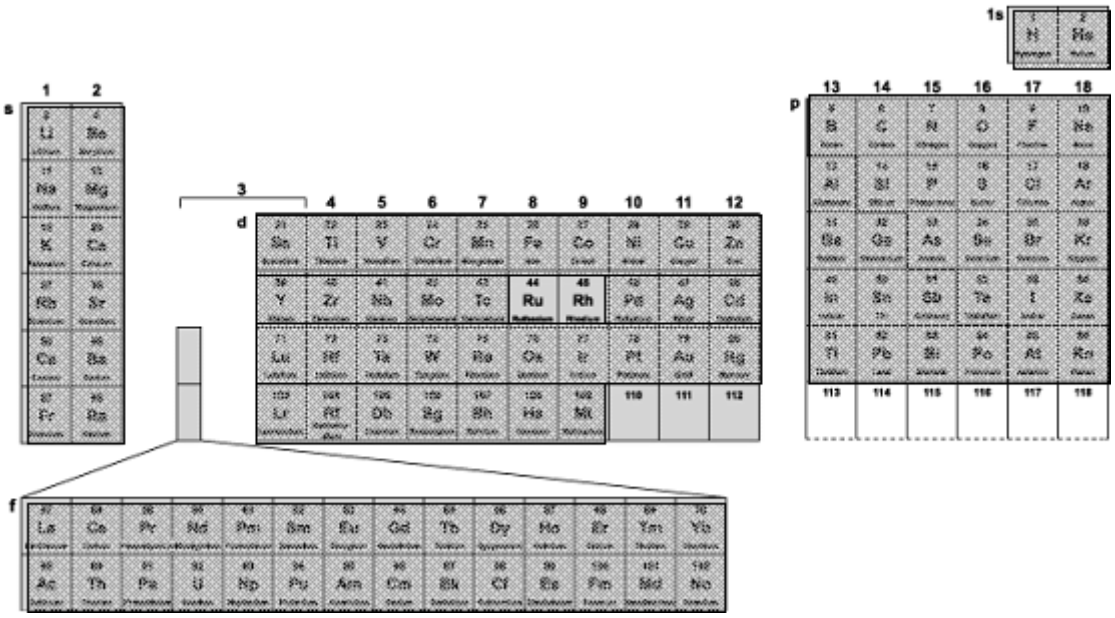

Figure 6

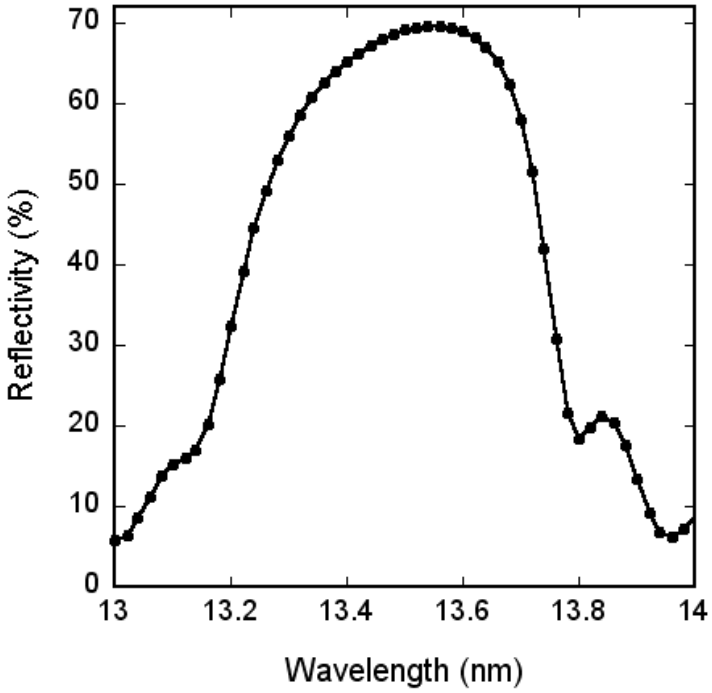
Reflectivity (%)
70
60
50
40
30
20
10
0
13
13.2
13.4
13.6
13.8
14
Wavelength (nm)

Figure 7

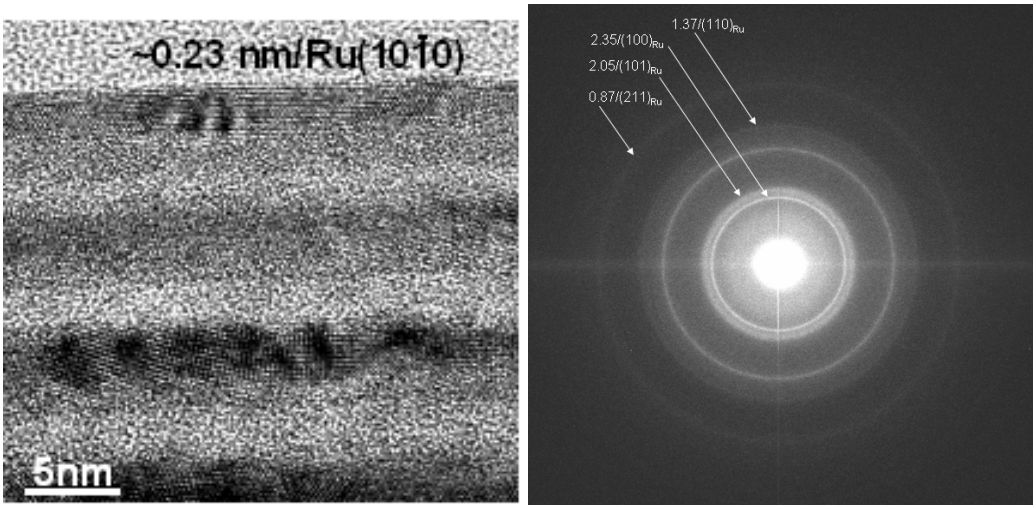

Figure 8

Tables

Table 1:

	R(Si)=	73.675				
Symbol		cap = 2nm		**cap=3 nm**		**cap = 4 nm**
	Rmax	R(Si) - Rmax	Rmax	R(Si)-Rmax	Rmax	R(Si)-Rmax
Be	73.769	**-0.09**	73.576	**0.10**	73.159	**0.52**
B	74.074	**-0.40**	73.726	**-0.05**	72.704	**0.97**
C	73.928	**-0.25**	73.139	**0.54**	71.462	**2.21**
Si	73.490	**0.19**	73.099	**0.58**	72.610	**1.07**
P	73.753	**-0.08**	73.432	**0.24**	72.823	**0.85**
S	73.669	**0.01**	73.154	**0.52**	72.220	**1.46**
Ca	73.693	**-0.02**	73.193	**0.48**	72.260	**1.41**
Sc	73.479	0.20	72.108	1.57	69.873	3.80
Ti	73.419	**0.26**	71.468	**2.21**	68.248	**5.43**
V	72.569	**1.11**	69.131	**4.54**	63.879	**9.80**
Mn	72.243	**1.43**	68.093	**5.58**	61.853	**11.82**
Rb	73.770	**-0.09**	73.700	**-0.03**	73.498	**0.18**
Sr	73.869	**-0.19**	73.761	**-0.09**	73.397	**0.28**
Y	74.142	**-0.47**	74.049	**-0.37**	73.482	**0.19**
Zr	74.408	**-0.73**	74.275	**-0.60**	73.405	**0.27**
Nb	74.873	**-1.20**	74.823	**-1.15**	73.736	**-0.06**
Tc	74.822	**-1.15**	74.047	**-0.37**	71.702	**1.97**
Ru	74.811	**-1.14**	73.599	**0.08**	70.590	**3.08**
Rh	73.800	**-0.13**	70.914	**2.76**	65.701	**7.97**
Pd	72.513	**1.16**	67.831	**5.84**	60.613	**13.06**
Ba	72.564	**1.11**	70.866	**2.81**	69.045	**4.63**
La	72.859	**0.82**	71.464	**2.21**	69.861	**3.81**
Ce	72.774	**0.90**	71.317	**2.36**	69.696	**3.98**
Pr	73.308	**0.37**	72.041	**1.63**	70.174	**3.50**
Nd	72.961	**0.71**	70.841	**2.83**	67.759	**5.92**
Pm	72.834	**0.84**	70.605	**3.07**	67.456	**6.22**
Sm	72.481	**1.19**	69.610	**4.07**	65.677	**8.00**
Eu	72.802	**0.87**	70.603	**3.07**	67.547	**6.13**
U	73.603	**0.07**	72.501	**1.17**	70.570	**3.11**

Table 2:

	R(Si) =	73.675	R(Si) =	73.675	R(Si) =	73.675
Compound	Rmax	cap = 2nm R(Si) - Rmax	Rmax	cap = 3nm R(Si) - Rmax	Rmax	cap = 4nm R(Si) - Rmax
B4C	74.07	**-0.40**	73.59	**0.09**	72.32	**1.36**
BeO	72.91	**0.77**	70.31	**3.37**	66.43	**7.24**
BN	73.68	**-0.01**	72.51	**1.16**	70.38	**3.29**
C22H10N2O5	73.68	**0.00**	72.81	**0.87**	71.22	**2.45**
C3H6	73.93	**-0.25**	73.67	**0.01**	73.00	**0.68**
C5H8O2	73.69	**-0.01**	72.91	**0.77**	71.48	**2.20**
C16H14O3	73.75	**-0.08**	73.11	**0.57**	71.86	**1.82**
C16H14O3	73.75	**-0.08**	73.11	**0.57**	71.86	**1.82**
C10H8O4	73.62	**0.05**	72.66	**1.02**	70.95	**2.73**
C8H7Cl	73.85	**-0.18**	73.44	**0.24**	72.51	**1.17**
C8H8	73.90	**-0.23**	73.52	**0.15**	72.68	**1.00**
Co2O3	72.65	**1.02**	67.05	**6.62**	59.31	**14.36**
MoO2	73.62	**0.05**	71.57	**2.10**	68.04	**5.64**
MoO3	73.41	**0.26**	71.35	**2.32**	67.99	**5.69**
MoSi2	74.02	**-0.34**	73.60	**0.08**	72.51	**1.17**
Ru2Si3	73.97	**-0.29**	73.03	**0.65**	71.06	**2.62**
RuO4	74.75	**-1.07**	72.73	**0.94**	69.54	**4.14**
SiC	73.61	**0.07**	72.89	**0.79**	71.65	**2.03**
Si3N4	73.36	**0.31**	71.89	**1.78**	69.60	**4.08**
SiO2	73.07	**0.61**	71.24	**2.44**	68.58	**5.09**
SiO2	72.95	**0.72**	70.81	**2.87**	67.69	**5.99**
TiN	73.36	**0.31**	70.92	**2.76**	66.90	**6.77**
TiO2	72.86	**0.81**	69.84	**3.83**	65.09	**8.59**
Si.925Ti.075O2	73.08	**0.60**	71.25	**2.43**	68.57	**5.10**
UO2	73.09	**0.58**	70.83	**2.84**	67.40	**6.27**
ZrO2	73.51	**0.16**	71.57	**2.10**	68.33	**5.34**

Appendix A

Multilayer and Capping Layer Development at LLNL: A Historical Perspective

Eberhard Spiller[2] first realized that high reflectivity normal incidence mirrors for extreme ultraviolet wavelengths can be made if one alternates materials of different absorption constants so that the absorber is placed into the nodes of the desired wave field. However, it took another 13 years to develop a high reflectivity EUV multilayer based on Mo/Si pair.[142] Since then lots of work has been done worldwide to optimize the multilayer properties and deposition parameters in order to increase the EUV reflectivity and to improve multilayer lifetime. In the following we are focusing on efforts done at LLNL between 1997 and 2002, when the first fully operational diffraction limited EUVL tool was demonstrated[143]. This work was done during the EUVL Cooperative Research and Development Agreement and funding was provided by the EUVLLC[56]. After 2003 most of the capping layer work at LLNL was funded by SEMATECH as part of LITH160 project.

In addition to optimizing the deposition parameters, chamber setup, chamber environment and starting materials (targets) to obtain the best performance of Mo/Si multilayers[144,145] considerable effort went into understanding other multilayer pairs (such as Mo/Be[146], MoRu/Be[147], Rh/Y and Mo_2C/Si). Be-based multilayers were of interest because the laser produced plasma source designed for EUVL had about four times higher output at 11.4 nm than at 13.5 nm. However, because of the smaller bandpass of 11.4 nm Mo/Be mirrors the integrated throughput was actually higher for the 13.5 nm

Mo/Si mirrors.[148] Considering also health and environmental risks the EUVL community declared 13.5 nm as the official EUVL wavelength. In order to maximize the optical throughput an increase in reflectivity and in the peak bandwidth of Mo/Si multilayers become very important. In parallel studies on thermal stability,[149] stress[150], and the effect of the substrate roughness[151] were performed together with different mitigation strategies. Studies on capping layer materials were initially exploring only material stability in the air and the performance of Si, Mo, Be, C, B_4C and Mo_2C layers was monitored as a function of time. It became clear that even under these conditions capping layer material thinner than 2 nm was ineffective to prevent oxidation of the multilayers, independent of material nanostructure.

The reflectivity of Mo/Si and Mo/Be multilayers decreased as a function of time. Si-terminated Mo/Si multilayers showed about 1% reflectance drop in one year while Be-terminated multilayers had about 1.2% reflectance drop over the same length of time. However, most of this reflectivity decrease occurred relatively soon after the deposition, within the first few weeks. The multilayers were stored in plastic (Fluorware) containers and some reflectivity drop could also be due to environmental contamination.

In 1998 we demonstrated 70% reflectivity Mo/Si multilayers using interface engineering.[9] Two different multilayer designs were studied: Mo/C/Si/C and $Mo/B_4C/Si/B_4C$ with the later better suppresing the interdiffusion between Mo and Si layers and resulting in higher reflectivity. In addition to the reflectivity we also studied their thermal stability and stress. We developed methods to reduce stress without

significant reflectance loss. The reflectivity of the B_4C-capped multilayers was not stable. Detailed Auger studies revealed that the stoichiometry of the B_4C deposited films changed as a function of depth and the presence of B_2O_3 on the surface was confirmed with XPS.

Si_3N_4 was identified as a promising material for a capping layer based on its optical constants. However, Si_3N_4 films exposed to an electron beam in presence of water vapor showed substantial increase in oxygen after the exposure.

Systematic radiation stability studies with EUV photons and electron beams started in 1998. Results from earlier research[152] suggested that the EUV radiation does not cause any significant damage to the multilayers but these experiments were made with low brightness EUV sources. However, when higher brightness EUV sources became available and the experiments were repeated at higher EUV doses we observed carbon deposition and enhanced oxidation of the surface layers.[153,3,4,5] Si-capped multilayers exposed to ozone, hydrogen peroxide or water (with no EUV light) showed no significant reflectivity loss. Indeed, exposure to hydrogen peroxide often led to increase in reflectivity of Si-capped multilayers, most likely due to cleaning of the surface (carbon). These experiments were performed on Mo/Si and Mo/Be multilayers with the last layer being Si or Be, respectively. In parallel, we were also developing methods for cleaning carbon contaminated optics.[6] It soon became obvious that there is a need for deeper understanding of the surface chemistry of multilayers exposed to the environment of the EUVL system.

Systematic experimental work on optics lifetime started in 2000. We demonstrated that Si-capped multilayers exposed to an electron beam (1-2 keV, 5μA/mm^2) oxidize and their reflectivity drops below acceptable level. First exposure experiments with Ru-capped multilayers were performed.[9] Ruthenium capping layers were deposited on Si, on Mo or on B_4C. Although a thinner Ru layer is desirable for high reflectivity it was determined experimentally that it has to be at least 2.2 nm thick to improve the reflectance stability. Initial results indicated that Ru deposited on Si with B_4C interface layer had the highest initial reflectivity and the best reflectance stability. However, these results were based on short exposure times (4-8 hrs) using an electron beam and low water vapor pressure (5 x 10^{-7} mbar). Longer exposures at higher water vapor pressures (2 x 10^{-6} mbar), corresponding to several months of operation in commercial EUVL tool environment showed visible changes on the Ru-capped multilayer surface. During long electron beam exposures the boron signal became smaller and finally disappeared. This was interpreted as a possible formation of boron hydrite escaping from the sample. The efforts to detect boron hydride during the electron beam exposures were fruitless. The amount of boron hydride was below detection limit and its mass overlaps with a much stronger peak from nitrogen.

In collaboration with Sandia National Laboratories lifetime stability testing using electron beams was carried out. Most of the tests were performed at a constant water vapor while varying the current density and the exposure times between 5 and 500 hours. The reflectance loss was correlated with the fluence but the scaling was not clear. A

collaboration with NIST at the end of 2002 provided new data on EUV exposures of Si- and Ru-capped multilayers although most of the work was still focused on Si-capped multilayers.[154] Preliminary results on Si- and Ru-capped multilayers based on accelerated EUV exposure, agreed well with the results obtained from accelerated electron beam exposures.[11] The study of Ru oxidation resistance and the microstructure was continued as part of the LITH160 project. The main goal was to determine the effect of the microstructure on the optics lifetime and to provide benchmark samples for world-wide EUVL community. A report[155] and a paper[12] describe the outcome of these studies. In addition a screening study for capping layer candidates, which revealed surprisingly different degradation mechanisms, was performed.[156.]

Appendix B

Reflectivity calculations

The reflectivity was calculated using our own software using densities (ρ), Delta (δ) and Beta (β) from the CXRO (Center for X-Ray Optics) web page.[79] To calculate the reflectivity we used the matrix formulation introduced by Abelés,[157] who wrote the chapter on multilayers in Born and Wolf's book.[158] The printout of the computer program is given in Spiller's book.[159] Results obtained with this software package agree with the results obtained using other methods[160] (recursive method) or other programs.[161,162]

The data in the tables were produced by calculating a reflectivity, R(λ), over a small wavelength range around λ = 13.5 nm and selecting the value at 13.5 nm as the output. In addition a 2nd degree polynomial was fitted through the 3 highest points of the R(λ) curve and the values of λ_{max} and R_{max} obtained from the fit were also added. The tables for the compounds were calculated by the same method. The results were compared to those obtained by the IMD[163] program and small differences, due to small differences in the optical constants from the CXRO website[79] and IMD package, were observed. Table B1 shows the optical constants obtained from the two sources. We found that the differences in the reflectivity values for the example of Table B1 are less than 0.1%.

Table B1: Optical constants for $\lambda = 13.5$ nm obtained from the CXRO web-site[79] and from Windt's IMD[163] program. A linear interpolation between the closest neighbors in the Windt's table was used to obtain values for 13.5 nm.

Material	n CXRO	k CXRO	n Windt	k Windt
Mo	0.92379312	0.006435488	0.92125	0.0064086
Si	0.9990021531	0.001826495	0.99936	0.0017161
TiO_2	0.94159918	0.002249589	0.94211	0.0024369

Appendix C

Reflectivity Calculations for Elements and Compound Materials "Deposited" on Mo- and Si-Terminated Multilayers

This section features results from reflectivity calculations for all of the materials under consideration. Table C1 features results for elemental materials deposited on a terminating layer of Mo; Table C2, results for elemental materials deposited on a terminating layer of Si; Table C3, results for compound materials on Mo and Table C4, results for compound materials on Si.

						R(Mo) =	74.97										
					cap = 2 nm					cap = 3 nm					cap = 4 nm		
Element	Density (g/cm3)	Delta	Beta	R(%) at 13.5 nm	λmax (nm)	Rmax	R(Mo) - Rmax	R(%) at 13.5 nm	λ max (nm)	Rmax	R(Mo) - Rmax	R(%) at 13.5 nm	λmax (nm)	Rmax	R(Mo) - Rmax
H	0.00008988	4.55048E-06	1.44654E-07	74.94	13.52	74.97	0.00	74.94	13.52	74.97	0.00	74.94	13.52	74.97	0.00
He	0.0001785	4.83785E-06	1.51537E-06	74.94	13.52	74.97	0.00	74.94	13.52	74.97	0.00	74.94	13.52	74.97	0.00
Li	0.534	0.009678403	0.010854666	69.48	13.52	69.51	5.46	67.90	13.50	67.90	7.07	67.48	13.48	67.51	7.46
Be	1.848	0.009601906	0.001536381	74.08	13.52	74.13	**0.84**	73.68	13.52	73.72	**1.25**	73.52	13.51	73.55	**1.42**
B	2.34	0.031632502	0.004065488	72.70	13.53	72.82	**2.15**	71.47	13.52	71.56	**3.41**	70.87	13.51	70.89	**4.08**
C	2.2	0.038426668	0.006905356	71.28	13.53	71.43	**3.54**	69.49	13.52	69.57	**5.40**	68.63	13.51	68.64	**6.33**
N	0.001251	2.3648E-05	7.00741E-06	74.93	13.52	74.97	0.00	74.93	13.52	74.97	0.00	74.93	13.52	74.96	0.01
O	0.001429	2.62557E-05	1.21564E-05	74.93	13.52	74.96	0.01	74.93	13.52	74.96	0.01	74.93	13.52	74.96	0.01
F	0.001696	2.882E-05	1.87759E-05	74.93	13.52	74.96	0.01	74.92	13.52	74.96	0.01	74.92	13.52	74.96	0.01
Ne	0.0008999	1.24215E-05	1.32338E-05	74.93	13.52	74.96	0.01	74.93	13.52	74.96	0.01	74.93	13.52	74.96	0.01
Na	0.971	0.009919077	0.015618929	67.23	13.52	67.25	7.72	65.10	13.49	65.12	9.85	64.58	13.47	64.69	10.28
Mg	1.738	0.007833125	0.027693361	61.85	13.51	61.85	**13.12**	58.61	13.45	58.83	**16.14**	57.93	13.42	58.52	**16.45**
Al	2.699	0.002844712	0.029659959	61.06	13.50	61.06	**13.91**	58.05	13.43	58.41	**16.56**	57.59	13.41	58.29	**16.68**
Si	2.33	0.000997847	0.001826495	73.99	13.52	74.02	**0.95**	73.73	13.51	73.75	**1.22**	73.68	13.51	73.69	**1.28**
P	2.2	0.012679263	0.002363718	73.64	13.52	73.70	**1.27**	73.07	13.52	73.10	**1.87**	72.84	13.51	72.86	**2.11**
S	2.05	0.014799886	0.003554353	73.03	13.52	73.11	**1.86**	72.24	13.52	72.27	**2.70**	71.95	13.51	71.96	**3.01**
Cl	0.003214	2.53092E-05	6.59455E-06	74.93	13.52	74.97	0.00	74.93	13.52	74.97	0.00	74.93	13.52	74.97	0.00
Ar	0.001784	1.33028E-05	4.00101E-06	74.94	13.52	74.97	0.00	74.93	13.52	74.97	0.00	74.93	13.52	74.97	0.00
K	0.862	0.007955141	0.00222072	73.74	13.52	73.79	1.18	73.29	13.51	73.32	1.66	73.13	13.51	73.14	1.83
Ca	1.55	0.015650302	0.003551432	73.03	13.52	73.11	**1.86**	72.22	13.52	72.25	**2.72**	71.91	13.51	71.92	**3.05**
Sc	2.989	0.030295767	0.00912289	70.23	13.53	70.34	4.63	68.32	13.51	68.34	6.63	67.55	13.50	67.56	7.41
Ti	4.54	0.048083212	0.014183081	67.82	13.53	68.00	**6.97**	64.77	13.52	64.81	**10.17**	63.38	13.49	63.40	**11.57**
V	6.11	0.056818146	0.021007055	62.97	13.54	63.20	**11.77**	58.31	13.51	58.32	**16.65**	56.25	13.44	56.53	**18.44**
Cr	7.19	0.06754794	0.038883127	57.39	13.56	57.73	**17.24**	50.96	13.50	50.96	**24.01**	48.11	13.37	49.18	**25.79**
Mn	7.3	0.067273036	0.031774044	60.24	13.55	60.56	**14.41**	54.51	13.51	54.52	**20.46**	51.85	13.41	52.40	**22.57**
Fe	7.874	0.060605358	0.052224226	52.31	13.56	52.65	**22.32**	45.09	13.41	45.33	**29.64**	42.34	13.31	44.79	**30.18**
Co	8.9	0.066652119	0.066206627	47.55	13.57	48.02	**26.95**	39.25	13.32	40.02	**34.95**	36.18	13.27	40.17	**34.80**
Ni	8.902	0.051776782	0.072721645	45.27	13.57	45.56	**29.41**	37.36	13.28	39.15	**35.82**	34.97	13.26	39.62	**35.35**
Cu	8.96	0.037569072	0.061354645	48.92	13.54	49.02	**25.95**	42.17	13.32	43.54	**31.43**	40.33	13.29	43.72	**31.26**
Zn	7.133	0.025479985	0.055495128	50.93	13.52	50.97	**24.00**	45.03	13.34	46.28	**28.69**	43.64	13.31	46.40	**28.57**
Ga	6.095	0.014839068	0.039337969	57.03	13.51	57.04	**17.93**	52.61	13.40	53.14	**21.83**	51.63	13.37	52.96	**22.02**
Ge	5.323	0.005334918	0.032092217	60.00	13.50	60.00	**14.97**	56.49	13.43	56.86	**18.11**	55.82	13.40	56.66	**18.31**
As	5.73	0.012148595	0.027029807	62.12	13.51	62.13	**12.84**	58.79	13.45	58.95	**16.02**	58.01	13.42	58.56	**16.42**
Se	4.5	0.005554568	0.014823136	67.62	13.51	67.64	**7.33**	65.71	13.49	65.73	**9.24**	65.29	13.47	65.38	**9.59**
Br	3.12	0.006475885	0.005875716	71.92	13.52	71.95	**3.02**	71.02	13.51	71.03	**3.94**	70.79	13.50	70.79	**4.18**
Kr	0.003733	-1.19465E-06	1.46934E-05	74.93	13.52	74.96	0.01	74.93	13.52	74.96	0.01	74.93	13.52	74.96	0.01
Rb	1.532	0.006076022	0.00072559	74.52	13.52	74.56	**0.41**	74.30	13.52	74.34	**0.63**	74.21	13.51	74.24	**0.73**
Sr	2.54	0.012302014	0.001337445	74.17	13.52	74.22	**0.75**	73.74	13.52	73.78	**1.19**	73.55	13.51	73.58	**1.39**
Y	4.457	0.026270168	0.00228152	73.61	13.52	73.73	**1.25**	72.76	13.52	72.86	**2.11**	72.33	13.52	72.36	**2.61**
Zr	6.506	0.042329926	0.003712155	72.85	13.53	73.01	**1.96**	71.44	13.53	71.57	**3.40**	70.65	13.52	70.69	**4.28**
Nb	8.57	0.066250637	0.005195977	72.11	13.54	72.37	**2.60**	69.95	13.54	70.20	**4.78**	68.55	13.52	68.65	**6.33**
Mo	10.22	0.076206878	0.006435488	71.53	13.54	71.85	**3.12**	68.96	13.54	69.26	**5.71**	67.22	13.53	67.33	**7.64**
Tc	11.5	0.093771182	0.012071688	68.98	13.55	69.42	**5.55**	65.10	13.55	65.49	**9.48**	62.44	13.52	62.52	**12.45**
Ru	12.1	0.113640599	0.017065153	66.93	13.56	67.59	**7.38**	61.83	13.57	62.47	**12.51**	58.10	13.53	58.22	**16.76**
Rh	12.41	0.124951787	0.03117277	61.20	13.58	62.11	**12.86**	53.86	13.58	54.63	**20.34**	48.76	13.51	48.76	**26.21**
Pd	12.02	0.12387988	0.045639102	55.39	13.59	56.50	**18.47**	46.43	13.59	47.14	**27.83**	40.75	13.44	41.45	**33.52**
Ag	10.5	0.109697357	0.079382524	44.19	13.61	45.62	**29.36**	33.54	13.60	33.82	**41.16**	28.31	13.22	33.66	**41.31**
Cd	8.65	0.071841091	0.054981146	51.45	13.57	51.93	**23.04**	43.58	13.43	43.69	**31.28**	40.31	13.30	42.99	**31.98**
In	7.31	0.069702379	0.070033453	46.34	13.58	46.88	**28.09**	37.73	13.31	38.66	**36.31**	34.52	13.26	38.94	**36.03**
Sn	7.3	0.058456402	0.072557919	45.39	13.57	45.77	**29.20**	37.18	13.29	38.71	**36.26**	34.49	13.26	39.17	**35.81**
Sb	6.691	0.054817941	0.06735675	47.04	13.57	47.35	**27.62**	39.21	13.31	40.48	**34.49**	36.67	13.27	40.77	**34.20**
Te	6.24	0.027154647	0.074921534	44.41	13.52	44.44	**30.54**	37.59	13.27	40.38	**34.59**	36.21	13.27	40.82	**34.15**
I	4.93	0.012135026	0.058274018	49.94	13.50	49.94	**25.03**	44.51	13.32	46.29	**28.68**	43.56	13.31	46.47	**28.50**
Xe	0.005887	-4.83128E-06	7.34338E-05	74.90	13.52	74.93	0.04	74.89	13.52	74.92	0.05	74.89	13.52	74.92	0.05
Cs	1.873	-0.006605171	0.01963372	65.49	13.50	65.49	**9.49**	63.47	13.46	63.58	**11.39**	63.19	13.45	63.43	**11.54**
Ba	3.5	-0.010575909	0.007047921	71.47	13.51	71.48	**3.50**	70.84	13.50	70.85	**4.13**	70.81	13.49	70.82	**4.15**
La	6.166	-0.003856285	0.006160412	71.85	13.51	71.87	**3.10**	71.17	13.50	71.17	**3.80**	71.07	13.50	71.07	**3.90**
Ce	6.771	-0.006488728	0.006238091	71.84	13.51	71.85	**3.12**	71.20	13.50	71.20	**3.77**	71.14	13.50	71.14	**3.83**
Pr	6.7	0.016851168	0.007337254	71.14	13.52	71.22	**3.75**	69.81	13.51	69.82	**5.15**	69.36	13.50	69.36	**5.61**
Nd	6.9	0.02597703	0.012779893	68.50	13.52	68.59	**6.38**	66.24	13.50	66.24	**8.73**	65.44	13.48	65.48	**9.49**
Pm	7	0.022198511	0.012987182	68.41	13.52	68.49	**6.48**	66.23	13.50	66.23	**8.74**	65.51	13.48	65.55	**9.42**
Sm	7.5	0.024209207	0.016907753	66.58	13.52	66.66	**8.31**	63.88	13.49	63.89	**11.08**	63.01	13.47	63.13	**11.84**
Eu	5.253	0.019140877	0.012495664	68.65	13.52	68.73	**6.25**	66.62	13.50	66.62	**8.35**	65.98	13.48	66.02	**8.95**
Gd	7.898	0.025824461	0.01876707	65.73	13.52	65.82	**9.16**	62.77	13.49	62.78	**12.19**	61.82	13.46	61.99	**12.99**
Tb	8.234	0.031459816	0.022134015	64.22	13.53	64.32	**10.65**	60.71	13.49	60.73	**14.24**	59.52	13.44	59.79	**15.18**
Dy	8.54	0.029376989	0.026895536	62.15	13.53	62.23	**12.74**	58.22	13.47	58.28	**16.69**	56.98	13.42	57.48	**17.49**
Ho	8.781	0.027603807	0.025522385	62.74	13.52	62.82	**12.15**	59.01	13.47	59.06	**15.91**	57.85	13.43	58.28	**16.69**
Er	9.045	0.02925862	0.026985902	62.11	13.53	62.19	**12.78**	58.18	13.47	58.24	**16.73**	56.94	13.42	57.44	**17.53**
Tm	9.314	0.027669484	0.028215287	61.58	13.52	61.66	**13.31**	57.59	13.47	57.68	**17.30**	56.38	13.42	56.95	**18.02**
Yb	6.7	0.015992343	0.021459362	64.55	13.52	64.58	**10.39**	61.62	13.48	61.67	**13.30**	60.84	13.45	61.13	**13.85**
Lu	9.835	0.029923111	0.027069461	62.07	13.53	62.16	**12.81**	58.11	13.47	58.17	**16.80**	56.85	13.42	57.36	**17.62**
Hf	13.31	0.038877066	0.034517787	58.97	13.53	59.09	**15.88**	53.99	13.46	54.10	**20.87**	52.31	13.39	53.25	**21.72**
Ta	16.65	0.057095058	0.040808279	56.56	13.55	56.81	**18.16**	50.34	13.47	50.39	**24.58**	47.88	13.36	49.22	**25.75**
W	19.3	0.067122005	0.032948803	59.76	13.55	60.08	**14.89**	53.91	13.51	53.92	**21.06**	51.23	13.40	51.85	**23.12**
Re	21.02	0.085099399	0.039895386	57.18	13.57	57.75	**17.22**	50.04	13.53	50.11	**24.86**	46.41	13.36	47.34	**27.63**
Os	22.57	0.096491121	0.043497425	55.97	13.58	56.69	**18.28**	48.11	13.55	48.27	**26.70**	43.86	13.34	44.94	**30.03**
Ir	22.42	0.095019594	0.044280838	55.65	13.58	56.36	**18.61**	47.77	13.55	47.91	**27.06**	43.57	13.34	44.75	**30.22**
Pt	21.45	0.109337643	0.060036976	50.32	13.60	51.40	**23.57**	40.72	13.58	41.04	**33.93**	35.54	13.27	38.32	**36.65**
Au	19.32	0.101221763	0.051750291	53.03	13.58	53.89	**21.08**	44.31	13.56	44.52	**30.45**	39.65	13.30	41.55	**33.42**
Hg	13.55	0.066655524	0.044553723	55.20	13.56	55.59	**19.39**	48.31	13.47	48.33	**26.64**	45.39	13.34	47.00	**27.97**
Tl	11.85	0.063129976	0.042125374	56.09	13.56	56.41	**18.57**	49.54	13.48	49.56	**25.41**	46.81	13.35	48.22	**26.75**
Pb	11.35	0.065294147	0.049113207	53.49	13.56	53.87	**21.10**	46.30	13.44	46.39	**28.58**	43.37	13.32	45.47	**29.50**
Bi	9.747	0.055704296	0.05533899	51.15	13.56	51.42	**23.55**	43.93	13.37	44.41	**30.56**	41.37	13.30	44.17	**30.81**
Po	9.32	0.048587542	0.055659566	50.98	13.55	51.17	**23.80**	44.05	13.36	44.73	**30.24**	41.78	13.30	44.62	**30.35**
Rn	9.73	3.60154E-05	7.33945E-05	74.90	13.52	74.93	**0.04**	74.89	13.52	74.92	**0.05**	74.89	13.52	74.92	**0.05**
Ra	5	0.009347029	0.04728299	53.95	13.50	53.95	**21.02**	49.23	13.36	50.28	**24.69**	48.37	13.35	50.31	**24.66**
Ac	10.07	-0.013492412	0.077766672	43.56	13.36	44.05	**30.92**	38.69	13.26	42.65	**32.32**	38.59	13.29	42.67	**32.30**
Th	11.72	0.000924771	0.042460017	55.83	13.49	55.83	**19.14**	51.77	13.38	52.67	**22.30**	51.14	13.36	52.67	**22.30**
Pa	15.37	-0.012808427	0.0121492	69.01	13.50	69.02	**5.96**	67.91	13.48	67.94	**7.03**	67.82	13.48	67.88	**7.09**
U	18.92	0.030313993	0.007818469	70.86	13.53	70.97	**4.00**	69.13	13.52	69.16	**5.81**	68.41	13.50	68.41	**6.56**

			R(Si)=	73.675								
Symbol	cap=2 nm				cap=3 nm				cap = 4 nm			
	R(%) at 13.5 nm	λ max (nm)	Rmax	R(Si) - Rmax	R(%) at 13.5 nm	λ max (nm)	Rmax	R(Si)-Rmax	R(%) at 13.5 nm	λ max (nm)	Rmax	R(Si)-Rmax
H	73.675	13.510	73.689	-0.01	73.675	13.510	73.688	-0.01	73.675	13.510	73.689	-0.01
He	73.675	13.510	73.689	-0.01	73.675	13.510	73.688	-0.01	73.674	13.510	73.688	-0.01
Li	72.549	13.529	72.714	0.96	70.322	13.541	70.640	3.04	67.571	13.545	67.919	5.76
Be	73.752	13.511	73.769	**-0.09**	73.547	13.515	73.576	**0.10**	73.119	13.517	73.159	**0.52**
B	74.059	13.510	74.074	**-0.40**	73.646	13.520	73.726	**-0.05**	72.570	13.527	72.704	**0.97**
C	73.898	13.515	73.928	**-0.25**	73.001	13.527	73.139	**0.54**	71.232	13.536	71.462	**2.21**
N	73.675	13.510	73.689	-0.01	73.674	13.510	73.687	-0.01	73.672	13.510	73.685	-0.01
O	73.674	13.510	73.688	-0.01	73.672	13.510	73.686	-0.01	73.668	13.510	73.682	-0.01
F	73.673	13.510	73.687	-0.01	73.670	13.510	73.683	-0.01	73.664	13.510	73.678	0.00
Ne	73.674	13.510	73.687	-0.01	73.671	13.510	73.685	-0.01	73.667	13.510	73.681	-0.01
Na	71.951	13.536	72.213	1.46	68.742	13.554	69.277	4.40	64.907	13.560	65.533	8.14
Mg	70.374	13.554	70.982	**2.69**	64.758	13.577	66.077	**7.60**	58.468	13.585	59.829	**13.85**
Al	69.761	13.560	70.559	**3.12**	63.529	13.582	65.047	**8.63**	56.916	13.588	58.350	**15.32**
Si	73.462	13.514	73.490	**0.19**	73.060	13.517	73.099	**0.58**	72.570	13.517	72.610	**1.07**
P	73.734	13.512	73.753	**-0.08**	73.391	13.517	73.432	**0.24**	72.742	13.521	72.823	**0.85**
S	73.641	13.514	73.669	**0.01**	73.070	13.521	73.154	**0.52**	72.111	13.524	72.220	**1.46**
Cl	73.675	13.510	73.689	-0.01	73.674	13.510	73.688	-0.01	73.672	13.510	73.686	-0.01
Ar	73.675	13.510	73.689	-0.01	73.674	13.510	73.688	-0.01	73.673	13.510	73.687	-0.01
K	73.615	13.513	73.638	0.04	73.231	13.517	73.272	0.40	72.625	13.520	72.677	1.00
Ca	73.666	13.514	73.693	**-0.02**	73.109	13.521	73.193	**0.48**	72.150	13.524	72.260	**1.41**
Sc	73.388	13.521	73.479	0.20	71.894	13.534	72.108	1.57	69.565	13.542	69.873	3.80
Ti	73.291	13.525	73.419	**0.26**	71.113	13.543	71.468	**2.21**	67.677	13.559	68.248	**5.43**
V	72.269	13.538	72.569	**1.11**	68.237	13.565	69.131	**4.54**	62.571	13.581	63.879	**9.80**
Cr	71.054	13.552	71.643	**2.03**	64.939	13.584	66.573	**7.10**	56.894	13.605	59.339	**14.34**
Mn	71.835	13.544	72.243	**1.43**	66.886	13.573	68.093	**5.58**	60.057	13.595	61.853	**11.82**
Fe	69.364	13.566	70.470	**3.21**	60.991	13.602	63.704	**9.97**	50.876	13.621	54.376	**19.30**
Co	68.100	13.574	69.635	**4.04**	57.913	13.612	61.549	**12.13**	46.082	13.637	50.685	**22.99**
Ni	66.864	13.582	68.799	**4.88**	55.351	13.619	59.665	**14.01**	42.720	13.643	48.016	**25.66**
Cu	67.536	13.577	69.184	**4.49**	57.158	13.612	60.818	**12.86**	45.756	13.633	49.930	**23.75**
Zn	67.731	13.575	69.273	**4.40**	57.869	13.609	61.226	**12.45**	47.193	13.625	50.850	**22.82**
Ga	69.214	13.565	70.232	**3.44**	61.681	13.594	63.781	**9.89**	53.358	13.606	55.707	**17.97**
Ge	69.747	13.561	70.575	**3.10**	63.258	13.584	64.897	**8.78**	56.174	13.594	57.832	**15.84**
As	70.602	13.552	71.163	**2.51**	65.209	13.575	66.460	**7.21**	59.036	13.584	60.372	**13.30**
Se	71.913	13.536	72.173	**1.50**	68.782	13.553	69.290	**4.39**	65.130	13.557	65.656	**8.02**
Br	73.094	13.521	73.185	**0.49**	71.879	13.528	72.030	**1.65**	70.338	13.530	70.501	**3.17**
Kr	73.673	13.510	73.687	-0.01	73.670	13.510	73.684	-0.01	73.666	13.510	73.680	0.00
Rb	73.756	13.510	73.770	**-0.09**	73.680	13.512	73.700	**-0.03**	73.473	13.514	73.498	**0.18**
Sr	73.856	13.510	73.869	**-0.19**	73.736	13.513	73.761	**-0.09**	73.358	13.517	73.397	**0.28**
Y	74.133	13.508	74.142	**-0.47**	74.019	13.515	74.049	**-0.37**	73.395	13.521	73.482	**0.19**
Zr	74.402	13.506	74.408	**-0.73**	74.233	13.517	74.275	**-0.60**	73.275	13.526	73.405	**0.27**
Nb	74.871	13.503	74.873	**-1.20**	74.777	13.518	74.823	**-1.15**	73.558	13.531	73.736	**-0.06**
Mo	74.989	13.503	74.991	**-1.32**	74.811	13.520	74.891	**-1.22**	73.354	13.535	73.573	**0.10**
Tc	74.808	13.510	74.822	**-1.15**	73.867	13.531	74.047	**-0.37**	71.253	13.551	71.702	**1.97**
Ru	74.784	13.513	74.811	**-1.14**	73.323	13.538	73.599	**0.08**	69.858	13.563	70.590	**3.08**
Rh	73.608	13.530	73.800	**-0.13**	70.084	13.564	70.914	**2.76**	64.092	13.589	65.701	**7.97**
Pd	72.036	13.547	72.513	**1.16**	66.226	13.583	67.831	**5.84**	57.764	13.610	60.613	**13.06**
Ag	68.353	13.574	69.915	**3.76**	57.824	13.615	61.736	**11.94**	45.091	13.644	50.738	**22.94**
Cd	69.461	13.566	70.567	**3.11**	60.999	13.603	63.781	**9.89**	50.606	13.623	54.318	**19.36**
In	67.818	13.576	69.459	**4.22**	57.212	13.614	61.078	**12.60**	44.977	13.641	50.076	**23.60**
Sn	67.137	13.580	68.990	**4.69**	55.852	13.618	60.058	**13.62**	43.269	13.643	48.563	**25.11**
Sb	67.542	13.577	69.238	**4.44**	56.839	13.614	60.719	**12.96**	44.800	13.640	49.492	**24.18**
Te	65.663	13.588	67.988	**5.69**	53.096	13.624	57.940	**15.73**	40.228	13.645	45.580	**28.10**
I	66.908	13.580	68.705	**4.97**	56.247	13.613	59.979	**13.70**	45.259	13.629	49.038	**24.64**
Xe	73.665	13.510	73.679	0.00	73.648	13.510	73.663	0.01	73.628	13.510	73.643	0.03
Cs	70.900	13.547	71.339	**2.34**	66.541	13.565	67.412	**6.26**	61.896	13.567	62.682	**10.99**
Ba	72.417	13.527	72.564	**1.11**	70.655	13.534	70.866	**2.81**	68.876	13.531	69.045	**4.63**
La	72.743	13.524	72.859	**0.82**	71.292	13.530	71.464	**2.21**	69.705	13.529	69.861	**3.81**
Ce	72.651	13.525	72.774	**0.90**	71.139	13.531	71.317	**2.36**	69.542	13.529	69.696	**3.98**
Pr	73.216	13.521	73.308	**0.37**	71.861	13.531	72.041	**1.63**	69.950	13.535	70.174	**3.50**
Nd	72.804	13.528	72.961	**0.71**	70.483	13.544	70.841	**2.83**	67.290	13.553	67.759	**5.92**
Pm	72.664	13.529	72.834	**0.84**	70.229	13.545	70.605	**3.07**	66.984	13.553	67.456	**6.22**
Sm	72.239	13.534	72.481	**1.19**	69.057	13.555	69.610	**4.07**	64.941	13.564	65.677	**8.00**
Eu	72.632	13.529	72.802	**0.87**	70.240	13.544	70.603	**3.07**	67.105	13.552	67.547	**6.13**
Gd	72.061	13.537	72.337	**1.34**	68.547	13.560	69.191	**4.48**	64.035	13.568	64.885	**8.79**
Tb	71.829	13.540	72.161	**1.51**	67.788	13.564	68.642	**5.03**	62.590	13.575	63.663	**10.01**
Dy	71.190	13.547	71.653	**2.02**	66.216	13.572	67.361	**6.31**	60.075	13.584	61.464	**12.21**
Ho	71.297	13.546	71.732	**1.94**	66.536	13.570	67.607	**6.07**	60.656	13.581	61.945	**11.73**
Er	71.175	13.547	71.642	**2.03**	66.182	13.572	67.333	**6.34**	60.024	13.585	61.419	**12.26**
Tm	70.976	13.549	71.486	**2.19**	65.721	13.574	66.958	**6.72**	59.327	13.587	60.805	**12.87**
Yb	71.415	13.543	71.797	**1.88**	67.171	13.565	68.056	**5.62**	62.092	13.572	63.079	**10.60**
Lu	71.187	13.547	71.652	**2.02**	66.193	13.572	67.346	**6.33**	60.021	13.585	61.424	**12.25**
Hf	70.605	13.555	71.237	**2.44**	64.500	13.582	66.072	**7.60**	57.003	13.601	59.077	**14.60**
Ta	70.497	13.558	71.206	**2.47**	63.803	13.588	65.648	**8.03**	55.360	13.608	57.958	**15.72**
W	71.699	13.545	72.136	**1.54**	66.549	13.575	67.825	**5.85**	59.510	13.597	61.396	**12.28**
Re	71.506	13.549	72.025	**1.65**	65.675	13.582	67.230	**6.44**	57.650	13.606	60.150	**13.52**
Os	71.484	13.550	72.033	**1.64**	65.391	13.584	67.066	**6.61**	56.944	13.609	59.694	**13.98**
Ir	71.355	13.552	71.932	**1.74**	65.107	13.586	66.841	**6.83**	56.519	13.610	59.336	**14.34**
Pt	70.217	13.563	71.191	**2.48**	62.124	13.602	64.805	**8.87**	51.554	13.626	55.531	**18.14**
Au	70.783	13.558	71.521	**2.15**	63.608	13.595	65.743	**7.93**	54.015	13.618	57.390	**16.28**
Hg	70.403	13.559	71.162	**2.51**	63.366	13.592	65.376	**8.30**	54.415	13.611	57.309	**16.37**
Tl	70.552	13.557	71.261	**2.41**	63.804	13.589	65.684	**7.99**	55.199	13.609	57.902	**15.77**
Pb	69.863	13.563	70.829	**2.85**	62.087	13.599	64.423	**9.25**	52.449	13.617	55.703	**17.97**
Bi	68.855	13.569	70.108	**3.57**	59.880	13.605	62.874	**10.80**	49.311	13.624	53.053	**20.62**
Po	68.565	13.571	69.892	**3.78**	59.338	13.606	62.439	**11.24**	48.688	13.625	52.445	**21.23**
Rn	73.666	13.510	73.680	**-0.01**	73.650	13.510	73.664	**0.01**	73.630	13.510	73.645	**0.03**
Ra	68.071	13.572	69.444	**4.23**	59.056	13.605	61.940	**11.74**	49.537	13.615	52.458	**21.22**
Ac	63.653	13.599	66.700	**6.98**	49.477	13.634	55.159	**18.52**	36.709	13.647	41.804	**31.87**
Th	68.331	13.570	69.589	**4.09**	59.899	13.601	62.475	**11.20**	51.134	13.609	53.625	**20.05**
Pa	71.670	13.536	71.933	**1.74**	68.752	13.548	69.177	**4.50**	65.773	13.546	66.115	**7.56**
U	73.551	13.519	73.603	**0.07**	72.327	13.530	72.501	**1.17**	70.313	13.538	70.570	**3.11**

Si/Mo

R(Mo) = 74.97

Formula	Density	Delta	Beta	cap = 2 nm R(%) at 13.5 nm	cap = 2 nm λ max (nm)	cap = 2 nm Rmax	cap = 2 nm R(Mo) - Rmax	cap = 3 nm R(%) at 13.5 nm	cap = 3 nm λ max (nm)	cap = 3 nm Rmax	cap = 3 nm R(Mo)-Rmax	cap = 4 nm R(%) at 13.5 nm	cap = 4 nm λ max (nm)	cap = 4 nm Rmax	cap = 4 nm R(Mo)-Rmax
AgBr	6.473	0.0446	0.0333	59.49	13.537	59.64	**15.33**	54.40	13.47	54.46	**20.52**	52.55	13.39	53.37	**21.60**
AlAs	3.810	0.0049	0.0243	63.33	13.508	63.34	**11.63**	60.51	13.46	60.66	**14.31**	59.94	13.43	60.36	**14.61**
Al2O3	3.970	0.0321	0.0390	57.16	13.528	57.24	**17.73**	52.06	13.43	52.35	**22.62**	50.55	13.37	51.84	**23.13**
AlP	2.420	0.0063	0.0138	68.11	13.513	68.13	**6.84**	66.29	13.49	66.31	**8.66**	65.88	13.47	65.95	**9.02**
B4C	2.520	0.0362	0.0051	72.15	13.528	72.29	**2.68**	70.66	13.52	70.75	**4.22**	69.93	13.51	69.94	**5.03**
BeO	3.010	0.0410	0.0173	66.40	13.531	66.54	**8.43**	63.15	13.51	63.15	**11.82**	61.84	13.47	61.93	**13.05**
BN	2.250	0.0373	0.0088	70.36	13.528	70.50	**4.47**	68.32	13.52	68.36	**6.61**	67.41	13.50	67.41	**7.56**
C22H10N2O5	1.430	0.0267	0.0063	71.61	13.524	71.72	**3.25**	70.18	13.52	70.22	**4.75**	69.59	13.50	69.59	**5.38**
C3H6	0.900	0.0200	0.0026	73.47	13.522	73.56	**1.41**	72.70	13.52	72.75	**2.22**	72.35	13.51	72.38	**2.60**
C5H8O2	1.190	0.0243	0.0056	71.95	13.523	72.05	**2.92**	70.67	13.52	70.70	**4.27**	70.14	13.50	70.14	**4.83**
C16H14O3	1.200	0.0234	0.0049	72.33	13.523	72.42	**2.55**	71.17	13.52	71.20	**3.77**	70.68	13.51	70.69	**4.28**
C16H14O3	1.200	0.0234	0.0049	72.33	13.523	72.42	**2.55**	71.17	13.52	71.20	**3.77**	70.68	13.51	70.69	**4.28**
C10H8O4	1.400	0.0268	0.0068	71.36	13.524	71.47	**3.50**	69.86	13.52	69.89	**5.08**	69.24	13.50	69.24	**5.73**
C2F4	2.200	0.0376	0.0202	65.09	13.53	65.22	**9.75**	61.61	13.50	61.61	**13.36**	60.30	13.46	60.48	**14.49**
C8H7Cl	1.290	0.0215	0.0036	72.98	13.523	73.07	**1.90**	72.04	13.52	72.08	**2.89**	71.63	13.51	71.65	**3.32**
C8H8	1.110	0.0222	0.0034	73.09	13.523	73.19	**1.78**	72.17	13.52	72.22	**2.75**	71.77	13.51	71.78	**3.19**
CaF2	3.180	0.0428	0.0209	64.78	13.533	64.93	**10.04**	61.06	13.50	61.06	**13.92**	59.58	13.45	59.76	**15.21**
CdWO4	7.900	0.0603	0.0345	59.08	13.549	59.35	**15.62**	53.32	13.49	53.32	**21.65**	50.87	13.39	51.66	**23.31**
CdS	4.826	0.0389	0.0257	62.66	13.531	62.78	**12.19**	58.52	13.49	58.54	**16.43**	57.03	13.43	57.42	**17.55**
CoSi2	5.300	0.0214	0.0222	64.20	13.521	64.26	**10.71**	61.01	13.48	61.05	**13.92**	60.09	13.44	60.39	**14.58**
Cr2O3	5.210	0.0637	0.0333	59.60	13.55	59.89	**15.08**	53.84	13.50	53.84	**21.13**	51.28	13.40	51.96	**23.01**
CsI	4.510	-0.0027	0.0502	52.89	13.477	52.91	**22.06**	48.54	13.35	50.00	**24.97**	48.00	13.34	50.10	**24.87**
CuI	5.630	0.0171	0.0572	50.31	13.505	50.32	**24.65**	44.71	13.33	46.28	**28.69**	43.60	13.31	46.45	**28.52**
InN	6.880	0.0726	0.0629	48.71	13.576	49.25	**25.72**	40.34	13.36	40.72	**34.25**	36.98	13.27	40.59	**34.38**
In2O3	7.179	0.0794	0.0674	47.32	13.585	47.99	**26.98**	38.42	13.34	38.81	**36.16**	34.73	13.26	38.83	**36.14**
InSb	5.775	0.0511	0.0568	50.60	13.554	50.83	**24.15**	43.50	13.36	44.18	**30.79**	41.12	13.30	44.08	**30.89**
GaAs	5.316	0.0121	0.0295	61.06	13.512	61.07	**13.90**	57.51	13.44	57.74	**17.23**	56.70	13.41	57.38	**17.59**
GaN	6.100	0.0317	0.0385	57.36	13.528	57.45	**17.53**	52.33	13.43	52.61	**22.37**	50.83	13.37	52.09	**22.88**
GaP	4.130	0.0143	0.0198	65.30	13.517	65.32	**9.65**	62.59	13.48	62.63	**12.34**	61.89	13.45	62.11	**12.86**
LiF	2.635	0.0456	0.0357	58.52	13.538	58.68	**16.29**	53.18	13.46	53.25	**21.72**	51.25	13.38	52.23	**22.74**
LiH	0.783	0.0174	0.0141	67.92	13.52	67.99	**6.98**	65.75	13.50	65.76	**9.21**	65.11	13.47	65.17	**9.80**
LiOH	1.430	0.0281	0.0166	66.69	13.525	66.79	**8.18**	63.91	13.50	63.91	**11.06**	62.95	13.47	63.05	**11.92**
MgO	3.580	0.0358	0.0465	54.27	13.532	54.36	**20.61**	48.47	13.39	48.98	**25.99**	46.75	13.34	48.68	**26.29**
Mg2Si	1.940	0.0058	0.0201	65.18	13.51	65.19	**9.78**	62.71	13.47	62.78	**12.19**	62.18	13.45	62.43	**12.54**
KAl3Si3O12H2	2.830	0.0280	0.0191	65.56	13.525	65.65	**9.32**	62.50	13.49	62.50	**12.47**	61.48	13.46	61.65	**13.32**
MnO	5.440	0.0614	0.0288	61.44	13.546	61.71	**13.26**	56.23	13.51	56.23	**18.74**	53.89	13.42	54.31	**20.66**
MnO2	5.030	0.0633	0.0296	61.11	13.548	61.40	**13.57**	55.75	13.51	55.75	**19.22**	53.31	13.42	53.76	**21.21**
MoO2	6.470	0.0659	0.0168	66.66	13.543	66.94	**8.03**	62.76	13.53	62.88	**12.10**	60.73	13.49	60.75	**14.22**
MoO3	4.690	0.0520	0.0153	67.33	13.536	67.52	**7.45**	64.02	13.52	64.08	**10.89**	62.47	13.48	62.50	**12.47**
MoSi2	6.310	0.0307	0.0043	72.57	13.526	72.69	**2.28**	71.32	13.52	71.41	**3.56**	70.73	13.51	70.75	**4.22**
NaCl	2.165	0.0190	0.0164	66.83	13.52	66.90	**8.07**	64.35	13.49	64.36	**10.61**	63.61	13.47	63.73	**11.24**
NiO	6.670	0.0567	0.0550	51.29	13.56	51.57	**23.40**	44.05	13.38	44.49	**30.48**	41.45	13.30	44.20	**30.77**
Ni2Si	7.200	0.0344	0.0486	53.49	13.531	53.58	**21.40**	47.61	13.38	48.25	**26.72**	45.93	13.33	48.05	**26.92**
Ru2Si3	6.960	0.0459	0.0084	70.57	13.532	70.74	**4.23**	68.38	13.52	68.48	**6.49**	67.30	13.50	67.30	**7.67**
SiC	3.217	0.0178	0.0048	72.40	13.521	72.48	**2.49**	71.38	13.51	71.40	**3.57**	70.99	13.51	71.00	**3.97**
Si3N4	3.440	0.0269	0.0093	70.14	13.524	70.24	**4.73**	68.30	13.51	68.31	**6.66**	67.60	13.49	67.60	**7.37**
SiO2	2.200	0.0220	0.0108	69.46	13.522	69.55	**5.43**	67.56	13.51	67.56	**7.41**	66.91	13.49	66.93	**8.04**
SiO2	2.650	0.0265	0.0130	68.40	13.524	68.50	**6.47**	66.10	13.50	66.11	**8.86**	65.29	13.48	65.34	**9.63**
TaN	16.300	0.0740	0.0436	55.62	13.564	56.09	**18.89**	48.54	13.50	48.54	**26.44**	45.31	13.34	46.75	**28.22**
TiN	5.220	0.0651	0.0192	65.58	13.544	65.85	**9.12**	61.38	13.53	61.47	**13.50**	59.26	13.47	59.32	**15.66**
Ta2Si	14.000	0.0450	0.0326	59.76	13.537	59.92	**15.05**	54.73	13.47	54.77	**20.20**	52.88	13.40	53.65	**21.32**
TiO2	4.260	0.0584	0.0225	64.11	13.542	64.35	**10.62**	59.71	13.52	59.73	**15.24**	57.68	13.45	57.85	**17.12**
Si.925Ti.075O2	2.205	0.0228	0.0109	69.41	13.523	69.49	**5.48**	67.47	13.51	67.47	**7.50**	66.80	13.49	66.82	**8.15**
UO2	10.960	0.0393	0.0150	67.42	13.53	67.56	**7.41**	64.50	13.51	64.51	**10.46**	63.31	13.48	63.36	**11.61**
H2O	1.000	0.0220	0.0077	70.93	13.523	71.02	**3.95**	69.41	13.51	69.43	**5.54**	68.86	13.50	68.86	**6.11**
Si.56Al.5P.16Li.04Ti.02Zr.02Zn.03O2.46	2.530	0.0251	0.0169	66.57	13.523	66.65	**8.32**	63.84	13.49	63.85	**11.12**	62.95	13.47	63.07	**11.90**
ZnO	5.675	0.0368	0.0450	54.85	13.533	54.95	**20.02**	49.12	13.40	49.54	**25.43**	47.38	13.34	49.18	**25.80**
ZnS	4.079	0.0195	0.0236	67.93	13.522	71.76	**3.21**	60.32	13.47	60.38	**14.59**	59.42	13.44	59.78	**15.19**
ZrO2	5.600	0.0537	0.0147	66.67	13.534	71.27	**3.70**	64.29	13.52	64.36	**10.61**	62.72	13.49	62.75	**12.23**
Y2O3	5.01	0.0428	0.0111	70.65	13.53	70.80	**4.17**	68.13	13.52	68.17	**6.80**	66.98	13.49	66.99	**7.98**
RuO2	6.97	0.0793	0.0215	65.97	13.55	66.34	**8.63**	61.03	13.54	61.17	**13.80**	58.24	13.47	58.30	**16.67**
RuO4	3.29	0.0419	0.0136	69.44	13.53	69.58	**5.39**	66.59	13.51	66.60	**8.37**	65.35	13.48	65.38	**9.59**
Co2O3	5.18	0.0551	0.0401	57.95	13.55	58.20	**16.77**	51.72	13.46	51.79	**23.18**	49.24	13.34	50.67	**24.31**
Co3O4	6.07	0.0630	0.0469	55.40	13.56	55.77	**19.20**	48.30	13.44	48.39	**26.58**	45.37	13.31	47.43	**27.54**

						R(Si) =	73.675			R(Si) =	73.675			R(Si) =	73.675
Compound	Density	Delta	Beta	R(%) at 13.5 nm	cap = 2 nm λ max (nm)	Rmax	R(Si) - Rmax	R(%) at 13.5 nm	cap = 3 nm λ max (nm)	Rmax	R(Si) - Rmax	R(%) at 13.5 nm	cap = 4 nm λ max (nm)	Rmax	R(Si) - Rmax
AgBr	6.473	0.0446	0.0333	70.93	13.55	71.50	**2.18**	65.18	13.58	66.63	**7.04**	57.92	13.60	59.82	**13.86**
AlAs	3.810	0.0049	0.0243	70.70	13.55	71.21	**2.46**	65.66	13.57	66.77	**6.90**	60.03	13.58	61.15	**12.53**
Al2O3	3.970	0.0321	0.0390	69.86	13.56	70.73	**2.94**	62.82	13.59	64.75	**8.92**	54.55	13.61	56.96	**16.72**
AlP	2.420	0.0063	0.0138	72.07	13.53	72.30	**1.37**	69.17	13.55	69.62	**4.05**	65.75	13.55	66.23	**7.45**
B4C	2.520	0.0362	0.0051	74.05	13.51	74.07	**-0.40**	73.49	13.52	73.59	**0.09**	72.15	13.53	72.32	**1.36**
BeO	3.010	0.0410	0.0173	72.71	13.53	72.91	**0.77**	69.79	13.55	70.31	**3.37**	65.64	13.57	66.43	**7.24**
BN	2.250	0.0373	0.0088	73.63	13.52	73.68	**-0.01**	72.32	13.53	72.51	**1.16**	70.08	13.54	70.38	**3.29**
C22H10N2O5	1.430	0.0267	0.0063	73.64	13.52	73.68	**0.00**	72.67	13.53	72.81	**0.87**	71.02	13.53	71.22	**2.45**
C3H6	0.900	0.0200	0.0026	73.91	13.51	73.93	**-0.25**	73.62	13.52	73.67	**0.01**	72.91	13.52	73.00	**0.68**
C5H8O2	1.190	0.0243	0.0056	73.65	13.52	73.69	**-0.01**	72.79	13.53	72.91	**0.77**	71.30	13.53	71.48	**2.20**
C16H14O3	1.200	0.0234	0.0049	73.72	13.51	73.75	**-0.08**	73.00	13.52	73.11	**0.57**	71.70	13.53	71.86	**1.82**
C16H14O3	1.200	0.0234	0.0049	73.72	13.51	73.75	**-0.08**	73.00	13.52	73.11	**0.57**	71.70	13.53	71.86	**1.82**
C10H8O4	1.400	0.0268	0.0068	73.58	13.52	73.62	**0.05**	72.50	13.53	72.66	**1.02**	70.73	13.54	70.95	**2.73**
C2F4	2.200	0.0376	0.0202	72.26	13.54	72.52	**1.15**	68.72	13.56	69.44	**4.23**	63.95	13.57	64.91	**8.77**
C8H7Cl	1.290	0.0215	0.0036	73.83	13.51	73.85	**-0.18**	73.36	13.52	73.44	**0.24**	72.39	13.53	72.51	**1.17**
C8H8	1.110	0.0222	0.0034	73.88	13.51	73.90	**-0.23**	73.47	13.52	73.52	**0.15**	72.57	13.52	72.68	**1.00**
CaF2	3.180	0.0428	0.0209	72.33	13.54	72.60	**1.08**	68.77	13.56	69.51	**4.17**	63.87	13.57	64.89	**8.79**
CdWO4	7.900	0.0603	0.0345	71.31	13.55	71.82	**1.86**	65.73	13.58	67.15	**6.52**	58.37	13.60	60.47	**13.21**
CdS	4.826	0.0389	0.0257	71.64	13.54	72.03	**1.65**	67.09	13.57	68.12	**5.56**	61.21	13.58	62.54	**11.14**
CoSi2	5.300	0.0214	0.0222	71.50	13.54	71.88	**1.80**	67.23	13.57	68.13	**5.54**	61.99	13.57	63.05	**10.63**
Cr2O3	5.210	0.0637	0.0333	71.56	13.55	72.02	**1.66**	66.27	13.58	67.59	**6.09**	59.14	13.60	61.06	**12.62**
CsI	4.510	-0.0027	0.0502	67.27	13.58	68.88	**4.79**	57.45	13.61	60.69	**12.98**	47.59	13.62	50.63	**23.04**
CuI	5.630	0.0171	0.0572	67.22	13.58	68.92	**4.76**	56.86	13.61	60.45	**13.22**	45.99	13.63	49.72	**23.95**
InN	6.880	0.0726	0.0629	68.66	13.57	70.02	**3.66**	59.09	13.61	62.42	**11.25**	47.70	13.63	52.04	**21.64**
In2O3	7.179	0.0794	0.0674	68.44	13.57	69.89	**3.78**	58.47	13.61	62.02	**11.65**	46.61	13.64	51.30	**22.38**
InSb	5.775	0.0511	0.0568	68.53	13.57	69.88	**3.80**	59.22	13.61	62.37	**11.31**	48.43	13.63	52.28	**21.39**
GaAs	5.316	0.0121	0.0295	70.30	13.56	70.94	**2.74**	64.44	13.58	65.86	**7.82**	57.80	13.59	59.31	**14.36**
GaN	6.100	0.0317	0.0385	69.90	13.56	70.76	**2.91**	62.94	13.59	64.84	**8.84**	54.75	13.61	57.12	**16.56**
GaP	4.130	0.0143	0.0198	71.57	13.54	71.91	**1.76**	67.61	13.56	68.40	**5.27**	62.87	13.57	63.75	**9.92**
LiF	2.635	0.0456	0.0357	70.69	13.55	71.32	**2.36**	64.55	13.58	66.15	**7.52**	56.88	13.60	59.06	**14.61**
LiH	0.783	0.0174	0.0141	72.38	13.53	72.59	**1.09**	69.64	13.55	70.08	**3.60**	66.15	13.56	66.67	**7.01**
LiOH	1.430	0.0281	0.0166	72.39	13.53	72.62	**1.06**	69.34	13.55	69.87	**3.81**	65.29	13.56	66.02	**7.66**
MgO	3.580	0.0358	0.0465	69.13	13.57	70.24	**3.44**	60.96	13.60	63.51	**10.16**	51.53	13.61	54.54	**19.14**
Mg2Si	1.940	0.0058	0.0201	71.25	13.54	71.64	**2.04**	67.05	13.56	67.90	**5.78**	62.25	13.57	63.12	**10.56**
KAl3Si3O12H2	2.830	0.0280	0.0191	72.08	13.54	72.36	**1.31**	68.55	13.56	69.25	**4.43**	63.96	13.57	64.84	**8.84**
MnO	5.440	0.0614	0.0288	71.99	13.54	72.35	**1.32**	67.42	13.57	68.49	**5.19**	61.08	13.59	62.66	**11.02**
MnO2	5.030	0.0633	0.0296	71.96	13.54	72.33	**1.34**	67.29	13.57	68.40	**5.28**	60.82	13.59	62.46	**11.22**
MoO2	6.470	0.0659	0.0168	73.50	13.53	73.62	**0.05**	71.17	13.55	71.57	**2.10**	67.26	13.56	68.04	**5.64**
MoO3	4.690	0.0520	0.0153	73.28	13.53	73.41	**0.26**	70.97	13.55	71.35	**2.32**	67.31	13.56	67.99	**5.69**
MoSi2	6.310	0.0307	0.0043	74.00	13.51	74.02	**-0.34**	73.51	13.52	73.60	**0.08**	72.37	13.53	72.51	**1.17**
NaCl	2.165	0.0190	0.0164	72.14	13.54	72.39	**1.29**	68.96	13.56	69.50	**4.17**	64.95	13.56	65.64	**8.03**
NiO	6.670	0.0567	0.0550	68.93	13.57	70.16	**3.51**	60.04	13.61	63.00	**10.68**	49.53	13.62	53.24	**20.43**
Ni2Si	7.200	0.0344	0.0486	68.84	13.57	70.04	**3.64**	60.30	13.60	63.03	**10.65**	50.58	13.62	53.74	**19.94**
Ru2Si3	6.960	0.0459	0.0084	73.93	13.52	73.97	**-0.29**	72.86	13.53	73.03	**0.65**	70.77	13.54	71.06	**2.62**
SiC	3.217	0.0178	0.0048	73.57	13.52	73.61	**0.07**	72.78	13.52	72.89	**0.79**	71.50	13.53	71.65	**2.03**
Si3N4	3.440	0.0269	0.0093	73.26	13.52	73.36	**0.31**	71.67	13.54	71.89	**1.78**	69.29	13.54	69.60	**4.08**
SiO2	2.200	0.0220	0.0108	72.93	13.53	73.07	**0.61**	70.95	13.54	71.24	**2.44**	68.22	13.55	68.58	**5.09**
SiO2	2.650	0.0265	0.0130	72.80	13.53	72.95	**0.72**	70.44	13.54	70.81	**2.87**	67.21	13.55	67.69	**5.99**
TaN	16.300	0.0740	0.0436	70.75	13.56	71.43	**2.24**	64.05	13.59	65.93	**7.75**	55.31	13.61	58.12	**15.55**
TiN	5.220	0.0651	0.0192	73.20	13.53	73.36	**0.31**	70.40	13.55	70.92	**2.76**	65.98	13.57	66.90	**6.77**
Ta2Si	14.000	0.0450	0.0326	71.03	13.55	71.57	**2.11**	65.40	13.58	66.80	**6.87**	58.26	13.60	60.11	**13.57**
TiO2	4.260	0.0584	0.0225	72.62	13.53	72.86	**0.81**	69.09	13.56	69.84	**3.83**	63.95	13.58	65.09	**8.59**
Si.925Ti.075O2	2.205	0.0228	0.0109	72.95	13.53	73.08	**0.60**	70.96	13.54	71.25	**2.43**	68.20	13.55	68.57	**5.10**
UO2	10.960	0.0393	0.0150	72.93	13.53	73.09	**0.58**	70.42	13.55	70.83	**2.84**	66.75	13.56	67.40	**6.27**
H2O	1.000	0.0220	0.0077	73.32	13.52	73.41	**0.27**	71.97	13.53	72.15	**1.52**	69.96	13.54	70.21	**3.47**
Si.56Al.5P.16Li.04Ti.022r.022n.03O2.46	2.530	0.0251	0.0169	72.26	13.53	72.50	**1.17**	69.09	13.56	69.64	**4.03**	64.97	13.56	65.71	**7.96**
ZnO	5.675	0.0368	0.0450	69.33	13.57	70.38	**3.29**	61.43	13.60	63.76	**9.92**	52.24	13.61	55.13	**18.55**
ZnS	4.079	0.0195	0.0236	71.26	13.55	71.69	**1.99**	66.68	13.57	67.68	**6.00**	61.16	13.58	62.30	**11.38**
ZrO2	5.600	0.0537	0.0147	73.39	13.52	73.51	**0.16**	71.21	13.54	71.57	**2.10**	67.68	13.56	68.33	**5.34**
Y2O3	5.01	0.0428	0.0111	74.95	13.52	75.04	**-1.37**	73.24	13.54	73.49	**0.18**	70.46	13.55	70.86	**2.82**
RuO2	6.97	0.0793	0.0215	74.73	13.53	74.90	**-1.22**	71.75	13.56	72.31	**1.37**	66.92	13.58	67.98	**5.69**
RuO4	3.29	0.0419	0.0136	74.62	13.53	74.75	**-1.07**	72.39	13.55	72.73	**0.94**	69.00	13.56	69.54	**4.14**
Co2O3	5.18	0.0551	0.0401	71.95	13.56	72.65	**1.02**	65.21	13.59	67.05	**6.62**	56.72	13.61	59.31	**14.36**
Co3O4	6.07	0.0630	0.0469	71.46	13.56	72.37	**1.30**	63.85	13.60	66.09	**7.58**	54.37	13.62	57.50	**16.18**

Appendix D

Concerning Reactivity of Elements with Oxygen

Table D1 contains useful data concerning the reactivity of various elements towards oxygen.[164] In general, if one considers any of the transition metal series (3d, 4d, 5d) of the periodic table, the reactivity is greatest on the left side, and decreases for elements to the right. Thus, Sc, Ti, Y, Zr, La, Hf all have high heats of oxide formation (i.e., they bond O strongly) while elements on the right side (Ni, Cu, Pd, Ag, Pt, Au) have low heats of oxide formation and bind O relatively weakly. The same trend is observed for reactivity of metals towards carbides and nitrides.[83] The heat of oxide formation is also the driving factor in the stability of H_2O interaction with surfaces. Transition elements on the left side dissociate H_2O aggressively, while those on the right do not: H_2O adsorbs in molecular form on Ni, Cu, Pd, Ag, Pt, and Au.

Table D1. Heats of Formation of Relevant Oxides

Useful table from V. E. Henrich and P. A. Cox, "The surface science of metal oxides" (Cambridge U. Press, 1994)

(Heat of formation of oxide ($-\Delta H_f$ in kJ per mole O)	Elements
0 – 50	Au, Ag. Pt
50 – 100	Pd, Rh
100 – 150	-
150 - 200	Ru, Cu
200 – 250	Re, Co, Ni
250 – 300	Na, Fe, Mo, Sn, Ge, W
300 – 350	Rb, Cs, Zn
350 – 400	K, Cr, Nb, Mn
400 – 450	V
450 – 500	Si
500 – 550	Ti, U, Ba, Zr
550 – 600	Al, Sr, La, Ce
600 – 650	Mg, Th, Ca, Sc

Appendix E

Film Materials References

Additional references on properties of various materials under consideration, where emphasis is given on materials that appeared promising optically but have not been investigated by LLNL.

BeO

T. Takagi, et al., J. Appl. Phys. **51**(10), 5419 (1980).

R.T. Chen, et al., Appl. Phys. Lett. **56**(8), 709 (1990).

BN

D.R. Strongin, et al., Appl. Phys. Lett. **60**(20), 2561 (1992).

H.F. Hofsass, et al., Appl. Phys. Lett. **67**(1), 46 (1995).

H.T. Tsou and W. Kowbel, Surface and Coatings Technology **79**, 139 (1996).

I. Jimenez, et al., Appl. Phys. Lett. **68**(20), 2816 (1996).

M. Lu, et al., Appl. Phys. Lett. **68**(5), 622 (1996).

J.A. Zapien, et al., Appl. Phys. Lett. **78**(14), 1982 (2001).

Y.H. Lu, et al., Appl. Phys. Lett. **87**, 151902 (2005).

L.J. Terminello, et al., J. Vac. Sci. Technol. A**12**, 2462 (1994).

S. Manorama, et al., J. Phys. D**26**, 1793 (1993).

P.B. Mirkarimi, et al., Appl. Phys. Lett. **66**, 2813 (1995).

A. Chaiken, et al., Appl. Phys. Lett. **63**, 2112 (1993).

Y. Kobayashi, et al., Jpn. J. Appl. Phys. **29**, 1004 (1990).

A.T. Bell, Plasma-Assisted CVD, Proceedings of the 8th International Conference on Chemical Vapor Deposition, Gouvieux, France, The Electrochemical Society, Inc., Pennington, NJ, 1981, p. 185.

T.A. Friedmann, et al., Appl. Phys. Lett. **63**, 1342 (1993).

B.R. Stoner and J.T. Glass, Appl. Phys. Lett. **63**, 698 (1992).

R. Kohl, et al., Appl. Phys. Lett. **63**, 1792 (1993).

D.J. Kester, et al., J. Mater. Res. **8**, 1213 (1993).

D.L. Medlin, J. Appl. Phys. **76**, 295 (1994).

C. Weissmantel, Preparation, Structure and Properties of Hard Coatings in Thin Films from Free Atoms and Particles (Academic, New York, 1989), pp. 385-452

CaF_2

R.W. Fathauer, et al., Appl. Phys. Lett. **45**(5), 519 (1984).

G.N. Chaudhari, et al., Appl. Phys. Lett. **62**(8), 852 (1993).

CdS

H.S. Kwok, et al., Appl. Phys. Lett. **52**(13), 1095 (1988).

C.M. Dai, et al. Appl. Phys. Lett. **59**(25), 3273 (1991).

F. B. Micheletti and P. Mark, Appl. Phys. Lett. **10(**4), 136 (1967).

Co_2O_3/ CoO/ Co_3O_4

W. Estrada, et al., J. Appl. Phys. **74**(9), 5835 (1993).

C.F. Windisch Jr., et al., J. Appl. Phys. **92**(9), 5572 (2002).

J. Jansson, et al., J. Catal. **211**, 387 (2002).

M. Matsumiya, et al., J. of the Electrochem. Soc. **151**(1), H7 (2004).

L. Le Brizoual, et al., Appl. Phys. Lett. **86**, 112505 (2005).

L. Smardz, et al., J. Appl. Phys. **71**, 5199 (1992).

I. Tsukada, et al., J. Appl. Phys. **80**(10), 5691 (1996).

G.A. Carson, et al., J. Vac. Sci. Technol. A **14**(3), 1637 (1996).

S. Spagna, et al., J. Appl. Phys. **79** (8), 4926 (1996).

R.J. Kennedy, J. Appl. Phys. **79**(8), 4570 (1996).

Cr_2O_3

R. Cheng, Appl. Phys. Lett. **81**(11), 2109 (2002).

J.S. Parker, Phys. Rev. Lett. **88**, 196601 (2002)

A. Sokolov, Europhys. Lett. **58**, 448 (2002).

L. Zhang, J. Vac. Sci. Technol. A **15**(3), 1576 (1997).

P.S. Robbert, J. Vac. Technol. A **16**(3), 990 (1998).

V.M. Bermudez, J. Vac. Sci. Technol. A **19**(2), 576 (2001).

M. Shima, J. Appl. Phys. **91**(10), 7920 (2002).

C.M. Fu, J. Appl. Phys. **91**(10), 7143 (2002).

L. Zhang, J. Vac. Sci. Technol. A **15**(3), 1576 (1997).

P.S. Robbert, J. Vac. Technol. A **16**(3), 990 (1998)

R. Cheng, Appl. Phys. Lett. **78**(4), 521 (2001).

GaP

S.W. Choi, K.J. Bachmann, and G. Lucovsky, J. Vac. Sci. Technol. A **11**(3), 626 (1993).

S.W. Choi, K.J. Bachmann, and G. Lucovsky, J. Vac. Sci. Technol. B **10**(3), 1070 (1992).

Numerical Data and Functional Relationships in Science and Technology, edited by K.H. Hellwege (Springer, Berlin, 1982), Vol. **111/ 17a**, p. 494.

M. Yamada, J. Appl. Phys. **72**(8), 3670 (1992).

M. Yamada, J. Appl. Phys. **74**(10), 6435 (1993).

M. Sugira, et al., J. appl. Phys. **77**(8), 4009 (1995).

L. Wang, J.A. Wolk, E.E. Haller, J. W. Erikson, M. Cardona, T. Ruf, J.P. Silveira, and F. Briones, Appl. Phys. Lett. **70**(14), 1831 (1997).

F. Echeverria, et al., J. Electrochem. Soc. **145**(9), 3011 (1998).

P.C. Ricci, J. of Appl. Phys. **97**, 113522 (2005).

R.W. Tjerkstra, Electrochemical and Solid State Letters **9**(5), C81 (2006).

V.K. Dixit, et al., Appl. Phys. Lett. **88**, 083115 (2006).

J.A. Van Vechten, J. Electron. Mater. **4**, 1159 (1975).

S.R. Morrison, et al., J. Phys. C **6**, L223 (1973).

Y. Ohno, et al., Phys. Rev. B **54**(7), 4642 (1996).

Q. Wu, et al., Appl. Phys. Lett. **75**(26), 4064 (1999).

D.R. Gibson, et al., SPIE Window and Dome Technologies and Materials III **1760**, 178 (1992).

D.R. Gibson, et al., SPIE **2286**, 335 (1994).

D.C. Harris, et al., SPIE **3060**, 17 (1997).

P. Klocek, et al., SPIE Window and Dome Technologies and Materials III **1760**, 210 (1992).

InN

Z.G. Qian, et al., J. Appl. Phys. **93**(5), 2643 (2003).

Z.G. Qian, et al., J. Appl. Phys. **92**(7), 3683 (2002).

J. Olia, et al., Appl. Phys. Lett **84**(9), 1486 (2004).

H.P. Zhou, et al., J. Appl. Phys. **96**(6), 3199 (2004).

T. Honke, et al., J. Vac. Sci. Technol. A **22**(6), 2487 (2004).

H. Lu, et al., J. Appl. Phys. **96**(6), 3577 (2004).

K.M. Yu, et al., Appl. Phys. Lett. **86**, 071910 (2005).

A. Uedono, et al., J. Appl. Phys. **97**, 043514 (2005).

R. Intartaglia, et al., Appl. Phys. Lett. **86**, 142104 (2005).

E. Dimakis, et al.,. J. Appl. Phys. **97**, 113520 (2005).

J.W. Chen, et al., Appl. Phys. Lett. **87**, 041907 (2005).

P.A. Anderson, et al., J. Appl. Phys. **98**, 043903 (2005).

M.F. Wu, et al., J. Vac. Sci. Technol. A **24**(2), 275 (2006).

R. Ascazubi, et al., Appl. Phys. Lett. **88**, 112111 (2006).

R.P. Bhatta, et al., Appl. Phys. Lett. **88**, 122112 (2006).

R.E. Jones, et al., Phys. Rev. Lett. **96**, 125505 (2006).

K. Wang, et al., Appl. Phys. Lett. **79**(11), 1602 (2001).

R.E. Morjan, et al., Proc. SPIE **4430**, 310 (2001).

P.P. Chen, et al., Proc. SPIE **5774**, 29 (2004).

Z. Lilenthal-Weber, et al., "Relation between structural and optical properties of InN and $In_xGa_{1-x}N$ thin films," *Physics of Semiconductors: 27th International Conference on the Physics of Semiconductors, ed. Jose Menendez and Chris Van de Walle, (American Institute of Physics, 2005) p. 209.*

Rh

J. Gustafson, et al., Phys. Rev. B **71**, 115442 (2005).

S. Petersson, et al., J. Appl. Phys. **51**(11), 373 (1980).

C.S. Petersson, et al., J. Appl. Phys. **53**(7), 4866 (1982).

P.A. Psaras, et al., J. Appl. Phys. **55**(10), 3536 (1984).

P.A. Psaras, et al., Appl. Phys. Lett. **47**(3), 250 (1985).

E. Spiller, et al., Appl. Phys. Lett. **54**(23), 2293 (1989).

J.S. Cohan, et al., Appl. Phys. Lett. **60**(11), 1402 (1992).

C. Liu, et al., J. Vac. Sci. Technol. A **17**(5), 2741 (1999).

C. V. Macchioni, et al., J. Appl. Phys. **87**(9), 5395 (2000).

J. Yuhara, et al., Phys. Rev. B **67**, 195407 (2003).

D. Cao, et al., J. Electrochem. Soc. **153**(5), A869 (2006).

S. C. Jung, et al., Phys. Rev. B **72**, 205419 (2005).

S. K. Kwon, et al., Phys. Rev. B **72**, 235423 (2005).

Y. Abe, et al., Surface Science Spectra **8**(2), 117 (2002).

A. Goldoni, et al., Phys. Rev. B **63**, 035405 (2000).

M. A. Tomaz, et al., Phys. Rev. B **58**(17), 58 (1998).

H. Li, et al., Phys. Rev. B Rapid Communications **44**(3), 1438 (1991).

TaN

C.S. Kang, et al., J. Vac. Sci. Technol. B **21**(5), 2026 (2003).

S. Noda, et al., J. Vac. Sci. Technol. A **22**(2), 332 (2004).

S.M Aoudi, et al., J. Vac. Sci. Technol. A **22**(5), 1975 (2004).

D. Adams, et al., J. Vac. Sci. Technol. B **22**(5), 2345 (2004).

J.-Y. Tewg, et al., J. Electrochem. Soc. **152** (8), G617 (2005).

C. Ren, et al., Appl. Phys. Lett. **87**, 073506 (2005).

M. Kumar, et al., Proc. SPIE **6037**, 60371E-1 (2005).

N. D. Cuong, et al., J. Electrochem. Soc. **153** (2), G164 (2006).

N.D. Cuong, et al., J. Vac. Sci. Technol. B **24**(2), 682 (2006).

T. Hara, et al., Electrochem. And Solid State Lett. **5** (5), G36 (2002).

TiN

J.E. Greene, et al., Appl. Phys. Lett. **67**(20), 2928 (1995).

P. Patsalas, et al., J. Appl. Phys. **9**6(11), 6234 (2004).

M. Matsuoka, et al., J. Vac. Sci. Technol. A **23**(1), 137 (2005).

V. Lingwal, et al., J. Appl. Phys. **97**, 104902 (2005).

H. Soderberg, et al., J. Appl. Phys. **97**, 114327 (2005).

S. B. S. Heil, et al., J. Vac. Sci. Technol. A **23**(4), L5 (2005).

H.-Y. Chen, et al., J. Vac. Sci. Technol. A **23**(4), 1006 (2005).

C. Muratore, et al., J. Vac. Sci. Technol. A **24**(1), 25 (2006).

Y. K. Zhang, et al., Proc. SPIE **6029**, 60290H-1 (2005).

P. Khatua, et al., Phys. Rev. B **73**, 064408 (2006).

P. Prieto, et al., J. Vac. Sci. Technol. A **13**(6), 2819 (1995).

Y. Liu, et al., Rev. of Sci. Instruments **76**, 084902 (2005).

V_2O_5

J. Schoiswohl, et al., Phys. Rev. B **69**, 155403 (2004).

D.-H. Youn, et al., J. Vac. Sci. Technol. A **22**(3), 719 (2004).

F.Y. Gan, et al., J. Vac. Sci. Technol. A **22**(3), 879 (2004).

M. Soltani, et al., J. Vac. Sci. Technol. A **22**(3), 859 (2004).

J. Schoiswohl, et al., Phys. Rev. Lett. **92**(20), 206103-1 (2004).

E. B. Macak, et al., J. Vac. Sci. Technol. A **22**(4), 1195 (2004).

M.V. Ganduglia-Pirovana, et al., Phys. Rev. B **70**, 045422 (2004).

X.M. Xiong, et al., Appl. Phys. Lett. **88**, 132906 (2006).

C. Yada, et al., J. Electrochem. Soc. **153**(6), A1148 (2006).

O. Tchernyshyov, Phys. Rev. Lett. **93**(15), 157206-1 (2004).

M. Soltani, et al., Appl. Phys. Lett. **85**(11), 1958 (2004).

M.B. Takeyama, et al., J. Vac. Sci. Technol. A 22(5), 2542 (2004).

L. A. Zepeda-Ruiz, et al., Phys. Rev. B **70**, 060102(R) (2004).

R. Plachy, et al., Phys. Rev. B **70**, 064411 (2004).

J.Y. Suh, et al., J. Appl. Phys. **96**(2), 1209 (2004).

[1] G. E. Moore, "Cramming more components onto integrated circuits", Electronics 38 (8), 1965.

[2] E. Spiller, "Low-loss reflectivity coatings using absorbing materials", Appl. Phys. Lett. 20, 365-367 (1972).

[3] M.E. Malinowski et al.,Proc. SPIE **4688,** 442 (2002).

[4] M.E. Malinowski, SEMATECH Project LITH113: EUV Optics Contamination Control Gas Blend Carbon Mitigation Data and Final Report, Report to International SEMATECH, Project LITH113, Agreement 399509-OJ.

[5] M. Malinowski, P. Grunow, C. Steinhaus, M. Clift and L. Klebanoff, SPIE **4343,** 347 (2001).
[6] S. Graham et al., Proc. SPIE **4688, 431** (2002); also cf. S. Graham, C. Steinhaus, M. Clift and L. Klebanoff, J. Vac. Sci. Technol., B**20,** 2393 (2002).

[7] B. Mertens et al., Proc. SPIE **5037**, 95 (2003); also cf. N. Koster, B. Mertens, R. Jansen, A. Van de Runstraat, F. Stietz, M. Wedowski, H. Meiling, R. Klein, A. Gottwald, F. Scholze, M. Visser, R. Kurt, P. Zalm, E. Louis, A. Yakshin, Microelectron. Eng. **61-62,** 65 (2002).

[8] K. Hamamoto, T. Tanaka, T. Watanabe, N. Sakaya, M. Hosoya, T. Shoki, H. Hada, N. Hishinuma, H. Sugahara, H. Kinoshita, J. Vac. Sci. Technol., B**23, 247** (2005).

[9] S. Bajt, J. B. Alameda, T. W. Barbee Jr., W. M. Clift, J. A. Folta, B. Kaufmann, E. A. Spiller, "Improved reflectance and stability of Mo-Si multilayers", Opt. Eng. 41 (2002) 1797-1804..

[10] S. Bajt, H. N. Chapman, N. Nguyen, J. Alameda, J. C. Robinson, M. Malinowski, E. Gullikson, A. Aquila, C. Tarrio, S. Grantham, "Design and Performance of Capping Layers for EUV Multilayer Mirrors," in *Emerging Lithographic Technologies VII*, R. L. Engelstad, ed., *Proc. SPIE* **5037** (2003), 236-248.

[11] S. Bajt, H. N. Chapman, N. Nguyen, J. Alameda, J. C. Robinson, M. Malinowski, E. Gullikson, A. Aquila, C. Tarrio, S. Grantham, "Design and performance of capping layers for extreme-ultraviolet multilayer mirrors", Appl. Opt. 42 (2003) 5750-5758.

[12] S. Bajt, Z. R. Dai, E. J. Nelson, M. A. Wall, J. B. Alameda, N. Q. Nguyen, S. L. Baker, J. C. Robinson, J. S. Taylor, A. Aquila, N. V. Edwards, J. Microlithogr. Microfabr. Microsyst. 5 (2006) 023004.

[13] B. M. Mertens, N. Koster, R. Jansen, A. van de Runstraat, H. Werij, F. Stietz, M. Wedowski, H. Meiling, R. Klein, R. Thornagel, F. Scholze, G. Ulm, R. Kurt, P. Zalm, E. Louis, A. Yakshiun, in : ASET/SEMATECH Workshop on EUV Lithography, Matsue, 2001, O4-5.

[14] A. E. Yakshin, E. Louis, E. L. G. Maas, F. Bijkerk, R. Klein, F. Scholze, P. Zalm, F. Stietz, M. Wedowski, S. Muellender, B. Mertens, H. Meiling, in ASET/SEMATECH Workshop on EUV Lithography, Matsue, 2001, P6-6.

[15] S. Bajt, S. Hau-Riege, J. Alameda, F. Dollar, M. Chandhok, M. Fang, "Protective capping layer for EUVL optics using TiO_2", 4th International Extreme Ultraviolet Lithography Symposium, San Diego, California, November 7 – 10, 2005.

[16] A. M. Hawryluk and L. G. Seppala, , "Soft-x-ray projection lithography using an x-ray reduction camera", J. Vac. Sci. & Technol. **B6**, 2162-2166 (1988).

[17] H. Kinoshita, K. Kurihara, Y. Ishii, and Y. Torii, "Soft X ray reduction lithography using multilayer mirrors", J. Vac. Sci. Technol. **B7**, 1648-1651 (1989).

[18] D. G. Stearns, R. S. Rosen, and S. P. Vernon, "Multilayer Mirror Technology for Soft-X-Ray Projection Lithography", Appl Opt **32**, 6952-6960 (1993).

[19] OSA Proceedings on Soft X Ray Projection Lithography (Opt. Soc. Am., 1992).

[20] A. B. C. Walker, J. T. W. Barbee, R. B. Hoover, and J. F. Lindblom, "Soft x-ray images of the solar corona with a normal incidence Cassegrain multilayer telescope", Science 241, 1781-1787 (1988).

[21] L. Golub, M. Herant, K. Kalata, I. Lovas, G. Nystrom, E. Spiller, and J. Wilczynski, "Sub-arcsecond observations of the solar x-ray corona", Nature **344**, 842-844 (1990).

[22] TRACE: http://trace.lmsal.com

[23] SOHO: sohowww.nascom.nasa.gov

[24] N. M. Ceglio, D. P. Gaines, J. Trebes, A. M. Hawryluk, D. G. Stearns, and G. L. Howe, "X ray laser cavity experiments", Proc. SPIE **688**, 44-49 (1987).

[25] P. Kirkpatrick and A. V. Baez, "Formation of optical images with x-rays", J. Opt. Soc. Amer., 38 (1948) 766.

[26] D. L. Shealy, C. Wang, W. Jiang, L. Jin, and R. B. Hoover, "Design and analysis of a fast, two-mirror soft x-ray microscope", Proc. SPIE **1741**, 20-31 (1992).

[27] I. Lovas, W. Santy, E. Spiller, R. Tibbetts, and J. Wilczynski, "Design and assembly of a high resolution Schwarzschild microscope for soft x rays", Proc. SPIE **316**, 90-97 (1981).

[28] J. A. Trail and R. L. Byer, "Compact scanning soft-x-ray microscope using a laser-produced plasma source and normal-incidence multilayer mirrors", Opt. Lett. **14**, 539-541 (1989).

[29] R. P. Haelbich, in Scanned Image Microscopy, edited by E. A. Ash (Academic Press, London, 1980), p. 413-434.

[30] J. Kirz, C. Jacobsen, and M. Howells, "Soft-X-Ray Microscopes and Their Biological Applications", Quart Rev Biophys **28**, 33-130 (1995).

[31] H. C. Kang, G. B. Stephenson, C.Liu, R. Conley, A. T. Macrander, J. Maser, S. Bajt, H. N. Chapman, "High-efficiency diffractive x-ray optics from sectioned multilayers", Appl. Phys. Lett. 86 (2005) 151109.

[32] H. C. Kang, J. Maser, G. B. Stephenson, C. Liu, R. Conley, A. T. Macrander, S. Vogt, " Nanometer linear focusing of hard x rays by a multilayer Laue lens", Phys. Rev. Lett. 96 (2006)127401.

[33] S. Bajt, H. N. Chapman, E. Spiller, S. Hau-Riege, J. Alameda, A. J. Nelson, C. C. Walton, B. Kjornrattanawanich, A. Aquila, F. Dollar, E. Gullikson, C. Tarrio, S. Grantham, "Multilayers for next generation x-ray sources", Proc. SPIE **6586** (2007) 65860J-1 – 65860J-10.

[34] Chapman, HN; Barty, A; Bogan, MJ; Boutet, S; Frank, M; Hau-Riege, SP; Marchesini, S; Woods, BW; Bajt, S; Benner, H; London, RA; Plonjes, E; Kuhlmann, M; Treusch, R; Dusterer, S; Tschentscher, T; Schneider, JR; Spiller, E; Moller, T; Bostedt, C; Hoener, M; Shapiro, DA; Hodgson, KO; Van der Spoel, D; Burmeister, F; Bergh, M; Caleman, C; Huldt, G; Seibert, MM; Maia, FRNC; Lee, RW; Szoke, A; Timneanu, N; Hajdu, J, "Femtosecond diffractive imaging with a soft-X-ray free-electron laser", Nature - Phys. **2,** 839-843, (2006).

[35] Stefan P. Hau-Riege, Henry N. Chapman, Jacek Krzywinski, Ryszard Sobierajski, Saša Bajt, Richard A. London, Magnus Bergh, Carl Caleman, Robert Nietubyc, Libor Juha, Jaroslav Kuba, Eberhard Spiller, Sherry Baker, Richard Bionta, K. Sokolowski-Tinten. N. Stojanovic, Benjawan Kjornrattanawanich, Eric Gullikson, Elke Plönjes, and Sven Toleikis, and Thomas Tschentscher, "Sub-nanometer-scale measurements of the interaction of ultrafast soft x-ray free-electron-laser pulses with matter", Phys. Rev. Lett. 98 (2007) 145502.

[36] Henry N. Chapman, Stefan P. Hau-Riege, Michael J. Bogan, Saša Bajt, Anton Barty, Sébastien Boutet, Stefano Marchesini, Matthias Frank, Bruce W. Woods, W. Henry Benner, Richard A. London, Urs Rohner, Abraham Szöke, Eberhard Spiller, Thomas Möller, Christoph Bostedt, David A. Shapiro, Marion Kuhlmann, Rolf Treusch, Elke Plönjes, Florian Burmeister, Magnus Bergh, Carl Caleman[4], Gösta Huldt, M. Marvin Seibert, Janos Hajdu, submitted to Nature (2007).

[37] S. Bajt, H. N. Chapman, E. Spiller, S. Hau-Riege, J. Alameda, A. J. Nelson, C. C. Walton, B. Kjornrattanawanich, A. Aquila, F. Dollar, E. Gullikson, C. Tarrio, S. Grantham, Multilayers for next generation x-ray sources, Proc. SPIE 6586 (2007) 6586-182.

[38] S. Wurm, and C. Gwyn, EUV Lithography, Chapter 8 of Microlithography, 2nd ed., editor K. Suzuki, CRC Press/Taylor and Francis Informa Group, Boca Raton, Florida, USA (2006), to be published.

[39] Delaboudiniere, J.-P.; Artzner, G. E.; Brunaud, J.; Gabriel, A. H.; Hochedez, J. F.; Millier, F.; Song, X. Y.; Au, B.; Dere, K. P.; Howard, R. A.; Kreplin, R.; Michels, D. J.; Moses, J. D.; Defise, J. M.; Jamar, C.; Rochus, P.; Chauvineau, J. P.; Marioge, J. P.; Catura, R. C.; Lemen, J. R.; Shing, L.; Stern, R. A.; Gurman, J. B.; Neupert, W. M.; Maucherat, A.; Clette, F.; Cugnon, P.; van Dessel,E, "EIT: Extreme-Ultraviolet Imaging Telescope for the SOHO mission", Solar Physics **162**, 291-312 (1996).

[40] T. W. Barbee Jr., J. C. Rife, W. R. Hunter, M. P. Kowalski, R. G. Cruddace, and J. F. Seely, Long-term stability of a Mo/Si multilayer structure, Appl. Opt. 32 (1993), 4852-4854.

[41] K. Boller, R. P. Haelbich, H. Hogrefe, W. Jerk, and C. Kunz, Nucl. Instrum. Method. 208 (1983) 273.

[42] B. R. Müller, J. Feldhaus, F. Schäfers, F. Eggenstein, "Cleaning of carbon contaminated vacuum ultraviolet-optics: Influence on surface roughness and reflectivity", Rev. Sci. Instrum. 63 (1992) 1428-1431.

[43] F. Eggenstein, F. Senf, T. Zeschke, W. Gudat, „Cleaning of contaminated XUV-optics at BESSY II", NIM A 467-468 (2001) 325-328.

[44] E. Gubbini, G. Kommol, M. Schnürer, H. Schönagel, U. Eichmann, M. P. Kalashnikov, P. V. Nickles, F. Eggenstein, G. Reichardt, W. Sandner, „"On-line" cleaning of optical components in a multi-TW-Ti:Sa laser system", Vacuum 76 (2004) 45-49.

[45] W. K. Warburton, P. Pianetta, "In situ optical element cleaning with photon activated oxygen", NIM A 319 (1992) 240-243.

[46] R. W. C. Hansen, J. Wolske, D. Wallace, M. Bissen, „Cleaning of optical surfaces with photogenerated reactants", NIM A 347 (1994) 249-253.

[47] A. Barty and K. A. Goldberg, Proc. SPIE 5037, 450 (2003).

[48] M. Malinowski, C. Steinhaus, M. Clift, L. E. Klebanoff, S. Mrowka, R. Soufli, "Controlling contamination in Mo/Si multilayer mirrors by Si surface-capping modifications", Proc. SPIE 4688 (2002) 442-453.

[49] M. Malinowski, P. Grunow, C. Steinhaus, M. Clift and L. Klebanoff, SPIE **4343,** 347 (2001).

[50] S. Graham, C. Steinhaus, M. Clift and L. Klebanoff, J. Vac. Sci. Technol., B**20,** 2393 (2002).

[51] B. Mertens, B.Wolschrijn, R. Jansen, N. Koster, M. Weiss, M. Wedowski, R. Klein, R. Bock, R. Thornagel,"EUV time resolved studies on carbon growth and cleaning", Proc. SPIE **5037** (2003) 95-102.

[52] K. Hamamoto, T. Tanaka, T. Watanabe, N. Sakaya, M. Hosoya, T. Shoki, H. Hada, N. Hishinuma, H. Sugahara, H. Kinoshita, J. Vac. Sci. Technol., B**23, 247** (2005).

[53] K. Motai, H. Oizumi, S. Miyagaki, I. Nishiyama, A. Izumi, T. Ueno, Y. Miyazaki, and A. Namiki, "Atomic hydrogen cleaning of Ru-capped EUV multilayer mirror", Proc. SPIE **6517** (2007) 65170F-1 – 65170F8.

[54] T E. Madey, N. S. Faradzhev, B. V. Yakshinskiy and N. V. Edwards, " Surface phenomena related to mirror degradation in extreme ultraviolet (EUV) lithography", Appl. Surf. Sci **253** (2006) 1691-1708.

[55] H. Over, Y. B. He, A. Farkas, G. Mellau, C. Korte, M. Knapp, M. Chandhok, M. Fang, "Long-term stability of Ru-based protection layers in extreme ultraviolet lithography: A surface science approach", to J. Vac. Sci. Technol. B25, July/Aug 2007.

[56] Extreme Ultraviolet Limited Liability Corporation

[57] Y. Kakutani, et al., "Lifetime improvement of projection mirror with Ru capping layer for EUVL by irradiation atmosphere," Proc. 4th International Symposium on Extreme Ultraviolet Lithography, San Diego Nov 7-9, 2005. https://www.sematech.org/7470

[58] I. Nishiyama, "Model of Ru surface oxidation for the lifetime scaling of EUVL projection optics mirror," Proc. 4th International Symposium on Extreme Ultraviolet Lithography, San Diego Nov 7-9, 2005. https://www.sematech.org/7470

[59] H. Takase, "Characterization of capped multilayer mirrors using XPS, AES and SIMS," Proc. Of SPIE 5751, 1084 (2005).

[60] M. Ishino, et al., "Heat stability of Mo/Si multilayers inserted with compound layers," Surface and Coatings Technology **169-170**, 628 (2003).

[61] H. Meiling, et al., "Prevention of MoSi multilayer reflection loss in EUVL tools," Proc. of SPIE **4506**, 93 (2001).

[62] H.-J. Voorma, et al., "Temperature induced diffusion in Mo/Si multilayer mirrors," J. Appl. Phys**. 83**(9), 4700 (1998).

[63] J.F. Seely, et al., "Effect of oxygen atom bombardment on the reflectance of silicon carbide mirrors in the extreme ultraviolet region," Appl. Optics **32**(10), 1805 (1993).

[64] A.E. Rosenbluth, "Computer search for layer materials that maximize the reflectivity of multilayer mirrors," Revue Phys. Appl. **23**, 1599 (1988).

[65] D.L. Windt, "Stress, microstructure, and stability of Mo/Si, W/Si, and Mo/C multilayer films," J. Vac. Sci. Technol. A **18**(3), 980 (2000).

[66] T. Bottger, et al., "Thermal stability of Mo/Si multilayers with boron carbide interlayers, Thin Solid Films **444**, 165 (2003).

[67] D.L. Windt, "Experimental comparison of extreme ultra-violet multilayers for solar physics," Appl. Optics **43** (9), 1835 (2004).

[68] E. Spiller, "Reflective multilayer coatings for the far uv region," Appl. Optics **15**(10), 2333 (1976).

[69] E. Spiller, "Low-loss reflection coatings using absorbing materials," Appl. Phys. Lett. **20**(9), 365 (1972).

[70] B. L. Henke, E. M. Gullikson, and J. C. Davis, "X-ray interactions: photoabsorption, scattering, transmission, and reflection at E = 50 – 30,000 eV, Z = 1-92", Atomic Data and Nuclear Data Tables **54**,181 (1993).

[71] R. Soufli, and E. M. Gullikson, "Reflectance measurements on clean surfaces for the determination of optical constants of silicon in the extreme ultraviolet-soft-x-ray region", Appl. Opt. **36**, 5499 (1997).

[72] J. Hilfiker, "VUV Ellipsometry," *Handbook of Ellipsometry, ed. H. Tompkins and G. Irene (William Andrew Publishing, 2005)* pp. 721- 798.

[73] R. Soufli, and E. M. Gullikson, "Absolute photoabsorption measurements of molybdenum in the range 60-930 eV for optical constant determination", App. Opt. **37**, 1713 (1998).

[74] R. Soufli, S. Bajt, and E. M. Gullikson, "Optical constants of beryllium from photoabsorption measurements for x-ray optics applications", SPIE **3767**, 251 (1999).

[75]B. Sae-Lao, and R. Soufli, "Measurements of the refractive index of yttrium in the 50-1300 eV energy region", App. Opt. **41**, 73097316 (2002).

[76] C. Tarrio, R. N. Watts, T. B. Lucatorto, J. M. Slaughter, and C. M. Falco, "Optical constants of in situ-deposited films of important extreme-ultraviolet multilayer mirror materials", Appl. Opt**. 37**, 4100 (1998).

[77] R. Soufli, "Optical constants of materials in the EUV/soft x-ray region for multilayer mirror applications", PhD Thesis, University of California Berkeley, December 1997.

[78] B. Kjornrattanawanich, "Reflectance, optical properties, and stability of molybdenum/strontium and molybdenum/yttrium multilayer mirrors", PhD Thesis, University of California Davis, 2002.
[79] http://www-cxro.lbl.gov/

[80] S. Bajt and E. Gullikson, private communication.

[81] B. L. Henke, E. M. Gullikson, and J. C. Davis, "X-ray interactions: photoabsorption, scattering, transmission, and reflection at E = 50 – 30,000 eV, Z = 1-92", Atomic Data and Nuclear Data Tables **54**, 181 (1993).

[82]A clarification on the use of the term "core electron:" it is quite common to refer to electrons in energy levels with binding energies greater than approx. 25 eV as core electrons. They are in shallow core levels, but core levels just the same. These localized electrons have binding energies considerably greater than the valence electrons that participate in chemical bonding (these have binding energies up to ~ 10eV).

[83] J. B. Benziger, "Thermodynamics of adsorption of diatomic molecules on transition metal surfaces", Appl. Surf. Sci. **6,** 105 (1980).

[84] T. E. Madey, F. M. Zimmermann, and R. A. Bartynski, *Proc. of Eighth Internat. Workshop on Desorption Induced by Electronic Transtitions (DIET 8),* Surf. Sci. **451**, 1-287 (2000).

[85] T. E. Madey, Surf. Sci. **299/300**, 824-836 (1994).

[86] L. Sanche, *Excess Electrons in Dielectric Media*, CRC Press, Boca Raton FL., 1-42 (1991).

[87] A. D. Bass and L. Sanche, Radiat. Phys. Chem. **68**, 3 (2003).

[88] M. L. Knotek and P. J. Feibelman, Surf. Sci. **90**, 78 (1979).

[89] T. Momose and H. Ishimaru, "Radiation damages in TRISTAN vacuum systems" J. Vac. Sci. Technol. A**9**, 2149 (1991).

[90] P. Rowntree, "Spectroscopic and desorption measurements of selective bond rupture in organic films", Surf. Sci. **390**, 70 (1997).

[91] V. Henrich and P. A. Cox, "The surface science of metal oxides" (Cambridge U. Press, 1994).

[92] Y. B. He, A. Goriachko, C. Korte, A. Farkas, G. Mellau, P. Dudin, L. Gregoriatti, A. Barinov, M. Kiskinova, A. Stierle, N. Kasper, S. Bajt, and H. Over, "Oxidation and reduction of ultrathin nano-crystalline Ru films on silicon: a model system for Ru-capped EUVL optics", accepted in JPC (2007).

[93] U. Diebold, "The surface science of titanium dioxide", Surf. Sci. Rpts. **48,** 53 (2003).

[94] R. L. Kurtz, R. Stockbauer and T. E. Madey,"Angular Distributions of Ions Desorbing from TiO_2", Nucl. Instr. & Meth. B**13**, 518 (1986).

[95] K. Hermann, private communication.

[96] N. G. Saha and H. G. Tomkins, "Titanium nitride oxidation chemistry: an x-ray photoelectron spectroscopy study" J. Appl. Phys. **72**, 3072 (1992).

[97] H. W. Hwu and J. G, Chen, "Surface chemistry of transition metal carbides", Chem.Rev. **105**, 185 (2005).

[98] P. Soukiassian and F. Amy, "Silicon carbide surface oxidation and SiO2/SiC interface formation investigated by soft x-ray synchrotron radiation", J. Electron Spectr. and Rel. Phenomena **144-147,** 783 (2005).

[99] Jung-Hwan Oh, Byung-Jun Oh, Doo-Jin Choi, Geung-Ho Kim and Hue-Sup Song "The effect of input gas ratio on the growth behavior of chemical vapor deposited SiC films", Journal of Materials Science **36**, 1695 (2001).

[100] M. L. Knotek, "Stimulated Desorption", Rept. Prog. Phys. **47**, 1499 (1984).

[101] T. E. Madey, R. Stockbauer, J. F. van der Veen, D. E. Eastman, "Angle-resolved photon-stimulated desorption of oxygen ions from a W(111) surface", Phys. Rev. Lett, **45**, 187 (1980).

[102] R. L. Kurtz, R. Stockbauer and T. E. Madey,"Angular Distributions of Ions Desorbing from TiO2", Nucl. Instr. & Meth. B**13**, 518 (1986).

[103] V. M. Bermudez and M. A. Hoffbauer, Phys Rev. B**30,** 1125 (1984).

[104] S. Tanaka, K. Mase, S. Nagaoka, and M. Kamada, Surf. Sci. 451 (2000) 182.

[105] E. Bertel, R. Stockbauer, R. L. Kurtz, D. E. Ramaker, T. E. Madey, "Resonant photoemission and the mechanism of photon-stimulated ion desorption in a transition metal oxide", Phys. Rev. B **31**, 5580 (1985).

[106] B. V. Yakshinskiy, R. Wasiliewski, E. Loginova, M. N. Hedhili, T. E. Madey, Surf. Sci. (2007), in press.

[107] R. Persaud and T. E. Madey, "Growth, Structure and Reactivity of Ultrathin Metal Films on TiO_2 Surfaces", in: *The Chemical Physics of Solid Surfaces and Heterogeneous Catalysis: Vol. 8, eds. D. A. King and D. P. Woodruff*, (Elsevier, Amsterdam, 1997). 407-447.

[108] W. Huang and W Ranke, "Autocatalytic partial reduction of FeO(111) and Fe3O4(111) films by atomic H", Surf. Sci. **600**, 793 (2006).

[109] http://www.webelements.com/webelements/scholar/

[110] S. Braun, H. Mai, M. Moss, R. Scholz, A. Leson, Jap. J. Appl. Phys. **41**, 4074-4081, 2002.

[111] S. Bajt, et al., "Benchmarking Reflectivity of EUV Multilayer Optics –Multilayer 1," SEMATECH Tech Transfer Document 03114453A-ENG, December, 2003.

[112] S. Bajt, et al., "Lifetime Benchmarking of EUV Multilayer Optics: Report on Screening Tests of Multilayer 2," Project Report for LITH160, 2004.

[113] E. Spiller and L. Golub, "Fabrication and testing of large area multilayer coated x-ray optics", Appl. Opt. **28**, 2969 (1989).

[114]S. Bajt and D. G. Stearns, "High-temperature stability multilayers for extreme-ultraviolet condenser optics", Appl. Opt. 44, 7735-7743, 2005.

[115]B. L. Henke, E. M. Gullikson, and J. C. Davis, "X-ray interactions: photoabsorption, scattering, transmission, and reflection at E = 50 – 30,000 eV, Z = 1-92", Atomic Data and Nuclear Data Tables 54, 181-343, 1993.

[116] R. Soufli, S. Bajt, and E. M. Gullikson, unpublished data.

[117] K. Hashimoto, H. Irie, A. Fujishima, "TiO2 photocatalysis: A historical overview and future prospects" Japan. J. Appl. Phys. 44 (2005) 8269-8285.

[118] K. Ro, W. Park, G. Choe, J. Ahn, Korean J. Mater. Res. **7**, 21 (1997).

[119] S. Bajt, S. Hau-Riege, Z. R. Dai, J. Alameda, E. Nelson, C. Evans, J. S. Taylor. F. Dollar, S. Hill, M. Chandhok, M. Fang, "Protective capping layer for EUVL optics using TiO_2", 2005 EUVL Symposium, San Diego, USA.

[120] S. Bajt, et al., "Lifetime Benchmarking of EUV Multilayer Optics: Report on Screening Tests of Multilayer 2," Project Report for LITH160, 2004.

[121] Workshop on EUV Optics Contamination and Lifetime, San Diego, Nov. 2005, unpublished.

[122] A. Atkinson, "Grain boundary diffusion in oxides and its contribution to oxidation processes," *Oxidation of Metals and Associated Mass Transport , ed. M.A. Dayananda, S.J. Rothman, W.E. King* (Metallurgical *Societ, Orlando, 1986)* pp. 29-47.

[123] N.L. Peterson, "Grain Boundary Diffusion in Metals," International Metals Reviews **28**(2), 65 (1983).

[124] C.A.J. Fisher and H. Matubara, "Oxide Ion Diffusion Along Grain Boundaries in Zirconia: A Molecular Dynamics Study, Solid State Ionics 113-115, 311 (1998); see also N. Bonanos, R.K. Slotwinski, B.C.H. Steele and E.P. Butler, J. Mater. Sci. Lett. **3**, 245 (1984).

[125] H. Haneda, I. Sakaguchi, A. Watanabe and J. Tanaka, "Oxygen Grain Boundary Diffusion in Zinc Oxide Ceramics," Defect and Diffusion Forum Vols. **143- 147**, 1219 (1997).

[126] U. Brossman, et al., "Oxygen diffusion in ultrafine grained monoclinic ZrO2," J. Appl. Phys. **85**(11), 7646 (1999).

[127] H.J. Hofler, et al., Defect Diffus. Forum **75**, 195 (1991).

[128] M.J. Verkerk, B.J. Middelhuis, and A.J. Burggraaf, Solid State Ionics **6**, 159 (1982).

[129] R. Vassen, D. Stover, et al., Brit. Ceram. Proc. **56**, 35 (1996).

[130] C.A.J. Fisher and H. Matubara, "Oxide Ion Diffusion Along Grain Boundaries in Zirconia: A Molecular Dynamics Study, Solid State Ionics 113-115, 311 (1998)

[131] U. Brossman, et al., "Oxygen diffusion in ultrafine grained monoclinic ZrO2," J. Appl. Phys. **85**(11), 7646 (1999).

[132] D. Gupta, D.R. Campbell, and P.S. Ho, "Grain boundary diffusion," *Thin Films—Interdiffusion and Reactions, ed. J.M. Poate, K.N. Tu, and J.W. Mayer, (Wiley-Interscience, Princeton, 1978), 161-242.*

[133] P. Gas, et al., "Grain boundary diffusion and segregation in bcc and fcc solid solutions," Eighth International Vacuum Congress **II**, 501 (1980).

[134] E.M. Lehockey, Mat. Res. Soc. Symp. Proc. **458**, 243 (1997).

[135] A.P. Zhilyaev, et al., Mat. Res. Soc. Symp. Proc. **458**, 61 (1997).

[136] S. Havlin, and D. Ben-Avraham, "Diffusion in Disordered Media," Advances in Physics **36**(6), 695 (1987).

[137] P. Guiraldenq, "Application of the percolation concept to the grain boundary diffusion mechanism," *Physical Chemistry of the Solid State: Applications to Metals and Their Compounds, ed. P. Lacombe, (Elsevier, Amsterdam, 1984), 215- 224.*

[138] Y. Limoge and J.L. Bocquet, "Temperature behavior of tracer diffusion in amorphous materials: a random walk approach," Phys. Rev. Lett. **65**(1), 60 (1990).

[139] D.S. Fisher, Phys. Rev. A **30**(2), 960 (1984).

[140] D.A. Neumayer, et al., J. Appl. Phys. 90(4), 1801 (2001), and private communication, N.V. Edwards, Freescale Semiconductor.

[141] K. Motai, H. Oizumi, S. Miyagaki, I. Nishiyama, A. Izumi, T. Ueno, Y. Miyazaki and A. Namiki, "Atomic hydrogen cleaning of Ru-capped EUV multilayer mirror", Proc. of SPIE Vol. 6517 (2007) p. 65170F.

[142] T. W. Barbee Jr., S. Mrowka, and M. C. Hettrick, "Molybdenum-silicon multilayer mirrors for the extreme ultraviolet", Appl. Opt. **24**, 883 (1985).

[143] H. N. Chapman, A.K. Ray-Chaudhuri, D. A. Tichenor, W. C. Replogle, R. H. Stulen, G. D. Kubiak, P.D. Rockett, L. E. Klebanoff, D. O'Connell, A. H. Leung, K. L. Jefferson, J. B. Wronsky, J. S. Taylor, L.

C. Hale, K. Blaedel, E. A. Spiller, G. E. Sommargren, J. A. Folta, D. W. Sweeney, , E. M. Gullikson, P. Naulleau, K. A. Goldberg, J. Bokor, D. T. Attwood, U. Mickan, R. Hanzen, E. Panning, P. Y. Yan. C. W. Gwyn, S. H. Lee, "First lithographic results from the extreme ultraviolet Engineering Test Stand", J. Vac. Sci. Technol. B19 (2001) 2389-2395.

[144] C. Montcalm, S. Bajt, P. B. Mirkarkimi, E. A. Spiller, F. J. Weber, and J. A. Folta, "Multilayer reflective coatings for extreme-ultraviolet lithography", Proc. SPIE **3331** (1998) 42-51.

[145] J. A. Folta, S. Bajt, T. W. Barbee Jr., R. F. Grabner, P. B. Mirkarimi, T. Nguyen, M. A. Schmidt, E. Spiller, C. C. Walton, M. Wedowski, and C. Montcalm, "Advances in multilayer reflective coatings for extreme-ultraviolet lithography", Proc. SPIE 3676 (1999) 702-709.

[146] S. Bajt, R. D. Behymer, P. B. Mirkarimi, C. Montcalm, M. A. Wall, M. Wedowski, and J. A. Folta, "Experimental investigation of beryllium-based multilayer coatings for extreme ultraviolet lithography", Proc. SPIE **3767** (1999) 259-270.

[147] S. Bajt, "Molybdenum-ruthenium/beryllium multilayer coatings", J. Vac. Sci. Technol. **A 18** (2000) 557-559.

[148] R. Stuik, Characterization of XUV Sources, Proefschrift, Technische Universiteit Eindhoven, Eindhoven (2002).

[149] P. B. Mirkarimi, "Stress, reflectance, and temporal stability of sputter-deposited Mo/Si and Mo/Be multilayer films for extreme ultraviolet lithography", Opt. Eng. **38** (1999) 1246-1259.

[150] C. Montcalm, "Reduction of residual stress in extreme ultraviolet Mo/Si multilayer mirrors with postdeposition thermal treatments", Opt. Eng. **40** (2001) 469-477.

[151] P. B. Mirkarimi, S. Bajt, and M. A. Wall, "Mo/Si and Mo/Be multilayer thin films on Zerodur substrates for extreme-ultraviolet lithography", Appl. Opt. **39** (2000) 1617-1625.

[152] D. Gaines, R. C. Spitzer, N. M. Ceglio, M. Krurey, G. Ulm, "Radiation hardness of molybdenum silicon multilayers designed for use in a soft x-ray projection lithography system", Appl. Opt. 32 (1993) 6991-6998.

[153] M. Wedowski, S. Bajt, J. A. Folta, E. M. Gullikson, U. Kleinberg, L. E. Klebanoff, M. E. Malinowski, W. M. Clift, "Lifetime studies of Mo/Si and Mo/Be multilayer coatings for extreme ultraviolet lithography", SPIE 3767 (1999) 217-224.

[154] C. Tarrio, S. Grantham, "Synchrotron beamline for extreme-ultraviolet multilayer mirror endurance testing", Rev. Sci. Instrum. 76 (2005) 056101.

[155] S. Bajt, et al., "Lifetime Benchmarking of EUV Multilayer Optics: Report on Screening Tests of Multilayer 2," Project Report for LITH160, 2004.

[156] S. Bajt, et al., "Benchmarking Reflectivity of EUV Multilayer Optics –Multilayer 1," SEMATECH Tech Transfer Document 03114453A-ENG, December, 2003.

[157] F. Abelés, Ann. de Physique **5,** "Recherches sur la propagation des ondes électromagnétique inusoidales dans les milieux stratifies. Application aux couches minces", 596-639 (1950).

[158] M. Born and E. Wolf, *Principles of Optics*, *5th ed*., (chapter 1.6) Pergamon Press, Oxford, 1975.

[159] E. Spiller, Soft X-ray Optics, (pp. 134) SPIE Optical Engineering Press, Bellingham, Washington, USA, 1994.

[160] P. Rouard, Annales de Physique **7,** "Études des propriétés optiques des lames métalliques très minces", 291-384 (1937).

[161] O. S. Heavens, *Optical Properties of Thin Solid Films* (Dover, New York, 1966).

[162] L. G. Parratt, Phys. Rev. **95,** "Surface studies of solids by total reflection of x rays", 359-368 (1954).

[163] D. L. Windt, "IMD- Software for modeling the optical properties of multilayer films", Computers in Physics 12 (1998), 360-370.

[164] V. E. Henrich and P. A. Cox, "The surface science of metal oxides" (Cambridge U. Press, 1994).